

Response to the reviewer' comments

We would like to thank the editor, associate editor and the reviewers for their insightful comments and suggestions, which helped improve this paper significantly. This paper has been revised according to the comments. All the comments have been addressed and responded to, as detailed in the point-by-point responses as below.

Some minor comments and potential areas of improvement:

1. Page 2, L29: “a lot” – not precise. Revise

Response:

Thanks.

The sentence has been changed as below:

'Interactions between precipitation products and hydrological models can have the similar magnitude of contribution to discharge uncertainty as the hydrological models.'

2. Page 3: remove bullets. Paragraph it!!

Response:

Thanks. They have been changed.

3. Page 4, L83: 3 citations are not many authors!!

Response:

Thanks. 'Many' has been deleted in the revised paper.

4. Pg 5, L112 – the aim stated here does not capture with clarity the thrust of the paper. The issues of coalitions and uncertainty are missing

Response:

Thanks. The statement has been changed as below:

'The overall objectives of this paper are: (1) to investigate the applicability of six fine-resolution precipitation products using both statistical and hydrological evaluation methods in a small river basin in northeast China; (2) to propose a framework to quantify the contributions of various uncertainties from precipitation products, hydrological models and their interactions to uncertainty in simulated discharges. The precipitation products investigated are TRMM3B42, TRMM3B42RT, GLDAS/Noah (GLDAS_Noah025SUBP_3H), APHRODITE, PERSIANN and GSMAP-MVK+.'

5. Pg 6, L140: “wholly” instead of “fully”

Response:

Thanks. It has been changed.

6. Pg 10, L243- Pg 11 L249: Consider putting this catchment description in section 2.1 (study area)

Response:

Thanks. They have been moved to the catchment description.

7. Pg 20,L467: “was” instead of “has been”

Response:

Thanks. It has been changed.

8. Pg 20,L468-9: Its not an issue of just comparing with other published parameter and then saying your parameters are acceptable. Shouldn't it be more about the system you are modelling compared to the other simialr systems published in papers?

Response:

Thanks. The sentence has been changed as below:

'Comparison with the rainfall-runoff model parameter values reported for the case study catchment in previous research shows the parameter values are appropriate (Qi et al., 2013;Qi et al., 2015, 2016).'

9. Pg 21, L512: 0.73 is not great performance. It seem more satisfactory than “great”. You can find information on how to interpret the range of NSE values on page 12555 of the first reference below or on page 8, section 3.3 of the second one

Response:

Thanks. It has been changed to 'satisfactory'.

10. Pg 21, L514: “This reveals the influence of different characterizations of...” What does this mean?

Response:

Thanks. This sentence has been revised as below:

'This reveals the influence of different combinations of hydrological models and precipitation data on discharge simulation, implying the accuracy does not solely depend on the accuracy of a precipitation produce.'

11. Pg 24, L580: "It is more complex.... More changeable" What is this "it"?

Response:

Thanks. 'It' has been deleted. The sentence has been changed as below:

'Middle magnitude discharges consist of contributions from base flows, lateral subsurface flows and overland flows, and can be triggered by rainfalls of various magnitudes - thus interactions are more variable.'

12. Pg 24, L586: Revise! Grammar!

Response:

Thanks. The sentence has been revised as below:

'precipitation products have a small contribution to the uncertainty in large discharges. This implies that the uncertainty in high precipitation is compensated by the high nonlinearity in hydrological models.'

13. Pg 25, L597: "The spatial...this study". What does that line mean?

Response:

Thanks. The sentence has been changed as below:

'The spatial variations in precipitation are not considered in this study.'

14. Pg 25, L614: Coalition and not collation, I think!!

Response:

Thanks. It has been changed to 'coalition'.

15. Pg 26, L618: "...tested in the future work" – delete "the"

Response:

Thanks. It has been deleted.

16. Pg 26, L629: compensation by

Response:

Thanks. It has been changed.

17. Pg 26, L630: modeling accuracy

Response:

Thanks. It has been changed.

18. Pg 26, L631-2: "That is, the errors... model processes". What does this mean? Could they be rather subsumed in model structural uncertainties?

Response:

Thanks. This sentence has been deleted.

19. Pg 27, L645: delete "be able to"

Response:

Thanks. It has been deleted.

20. Pg 27, L660-662: “At present... precipitation analysis” the GPM statement is hanging, not integrated! It sounds out of context! Revise!

Response:

Thanks. The sentence has been changed as below:

'At present, the NASA Global Precipitation Measurement (GPM) mission combines the artificial neural network function of PERSIANN and precipitation radar-matching of TRMM Multi-satellite Precipitation Analysis.'

References:

Qi, W., Zhang, C., Chu, J., and Zhou, H.: Sobol's sensitivity analysis for TOPMODEL hydrological model: A case study for the Biliu River Basin, China, Journal of Hydrology and Environment Research, 1, 1-10, 2013.

Qi, W., Zhang, C., Fu, G., and Zhou, H.: Global Land Data Assimilation System data assessment using a distributed biosphere hydrological model, JHyd, 528, 652-667, 10.1016/j.jhydrol.2015.07.011, 2015.

Qi, W., Zhang, C., Fu, G., and Zhou, H.: Quantifying dynamic sensitivity of optimization algorithm parameters to improve hydrological model calibration, JHyd, 533, 213-223, 10.1016/j.jhydrol.2015.11.052, 2016.

Evaluation of global fine-resolution precipitation products and their uncertainty quantification in ensemble discharge simulations

Wei Qi^{1,2}, Chi Zhang¹, Guangtao Fu², Chris Sweetapple² and Huicheng Zhou¹

¹ School of Hydraulic Engineering, Dalian University of Technology, Dalian 116024, China

² Centre for Water Systems, College of Engineering, Mathematics and Physical Sciences, University of Exeter, North Park Road, Harrison Building, Exeter EX4 4QF, UK

Correspondence to: Chi Zhang (czhang@dlut.edu.cn)

Abstract

The applicability of six fine-resolution precipitation products, including precipitation radar, infrared, microwave and gauge-based products using different precipitation computation recipes, is evaluated using statistical and hydrological methods in northeastern China. In addition, a framework quantifying uncertainty contributions of precipitation products, hydrological models and their interactions to uncertainties in ensemble discharges is proposed. The investigated precipitation products are TRMM3B42, TRMM3B42RT, GLDAS/Noah, APHRODITE, PERSIANN and GSMAP-MVK+. Two hydrological models of different complexities, i.e., a water and energy budget-based distributed hydrological model and a physically-based semi-distributed hydrological model, are employed to investigate the influence of hydrological models on simulated discharges. Results show APHRODITE has high accuracy at a monthly scale compared with other products, and GSMAP-MVK+ shows huge advantage and is better than TRMM3B42 in RB, NSE, RMSE, CC, false alarm ratio and critical success index. These findings could be very useful for

validation, refinement and future development of satellite-based products (e.g., NASA Global Precipitation Measurement). Although large uncertainty exists in heavy precipitation, hydrological models contribute most of the uncertainty in extreme discharges. **Interactions between precipitation products and hydrological models can have the similar magnitude of contribution to discharge uncertainty as the hydrological models.** A better precipitation product does not guarantee a better discharge simulation because of interactions. It is also found that a good discharge simulation depends on a good coalition of a hydrological model and a precipitation product, suggesting that, although the satellite-based precipitation products are not as accurate as the gauge-based product, they could have better performance in discharge simulations when appropriately combined with hydrological models. This information is revealed for the first time and very beneficial for precipitation product applications.

1 Introduction

Knowledge of precipitation plays an important role in the understanding of the water cycle, and thus in water resources management (Sellers, 1997; Sorooshian et al., 2005; Wang et al., 2005; Ebert et al., 2007; Buarque et al., 2011; Tapiador et al., 2012; Yong et al., 2012; Gao and Liu, 2013; Peng et al., 2014a; Peng et al., 2014b). However, precipitation data are not available in many regions, particularly mountainous districts and rural areas in developing countries. For example, Northeast China, which plays an important role in food production to support the country's population and is also an industrial region with many heavy industries, frequently suffers from drought, posing a threat to regional sustainable development. In such areas, due to insufficient gauge observations, alternative precipitation data are required for efficient water resources management.

In recent years, implementation of gauge-based and remote satellite-based precipitation products has become popular, particularly for ungauged catchments (Artan et al., 2007; Jiang et al., 2012; Li et al., 2013; Müller and Thompson, 2013; Maggioni et al., 2013; Xue et al., 2013; Kneis et al., 2014; Meng et al., 2014; Ochoa et al., 2014). Numerous precipitation products have been developed to estimate rainfall, for example: Tropical Rainfall Measuring Mission (TRMM) products (Huffman et al., 2007), Global Land Data Assimilation System (GLDAS) precipitation products (Kato et al., 2007), Asian Precipitation - Highly-Resolved Observational Data Integration Towards Evaluation of Water Resources (APHRODITE) (Xie et al., 2007; Yatagai et al., 2012), Precipitation Estimation from Remotely Sensed Information using Artificial Neural Networks (PERSIANN) (Sorooshian et al., 2000; Sorooshian et al., 2002), and Global Satellite Mapping of Precipitation product (GSMAP) (Kubota et al., 2007; Aonashi et al., 2009).

There are uncertainties in these products. Several studies have been carried out to analyze the uncertainty of TRMM in high latitude regions (Yong et al., 2010; Yong et al., 2012; Chen et al., 2013a; Yong et al., 2014; Zhao and Yatagai, 2014), but studies in northeast China are few. Evaluation of GLDAS data has generally been limited to the United States and other observation-rich regions of the world (Kato et al., 2007); assessments and applications in other regions are rare (Wang et al., 2011; Zhou et al., 2013). The APHRODITE, PERSIANN and GSMAP products are seldom evaluated in northeast China using basin scale gauge data (Zhou et al., 2008). Owing to the high heterogeneity of rainfall across a variety of spatiotemporal scales, the uncertainty characteristics of precipitation products are variable (Asadullah et al., 2008; Dinku et al., 2008; Nikolopoulos et al., 2010; Pan et al., 2010). Thus, in northeast China, it is essential to completely evaluate the applicability of these precipitation

products. In addition, it is also worth comparing the performance of different precipitation computation recipes: for example, the artificial neural network function used in PERSIANN, the histogram matching approach used in TRMM3B42, and the cloud motion vectors used in GSMAP-MVK+, because the inter-comparison could reveal the strategies that could be used to obtain more accurate precipitation data.

Many Researchers have implemented precipitation products in discharge simulations and reported discharge uncertainties (Hong et al., 2006;Pan et al., 2010;Serpetzoglou et al., 2010). Also, many uncertainty analysis approaches have been introduced to quantify the uncertainty (Beven and Binley, 1992;Freer et al., 1996;Kuczera and Parent, 1998;Beven and Freer, 2001b;Peters et al., 2003;Heidari et al., 2006;Kuczera et al., 2006;Tolson and Shoemaker, 2007;Blasone et al., 2008;Vrugt et al., 2009a;Vrugt et al., 2009b). In these prior approaches, one of the popular methods is the generalized likelihood uncertainty estimation (GLUE) technique, introduced by Beven and Binley (1992). This approach outputs probability distributions of model parameters conditioned on observed data, and the uncertainties in model inputs are represented by uncertain parameters. Similar to GLUE, Hong et al. (2006) proposed a Monte Carlo based method to quantify uncertainty in hydrological simulations using satellite precipitation data, in which flow simulation uncertainty is represented by ensemble simulation results.

In addition to individual contributions from hydrological models and precipitation data, the interactions between precipitation products and hydrological models also contribute to uncertainty in simulated discharges. However, to the best of our knowledge, the previous studies have not quantified the respective contributions of precipitation products, hydrological models and their interactions to the total discharge simulation uncertainty.

The overall objectives of this paper are: (1) to investigate the applicability of six fine-resolution precipitation products using both statistical and hydrological evaluation methods in a small river basin in northeast China; (2) to propose a framework to quantify the contributions of various uncertainties from precipitation products, hydrological models and their interactions to uncertainty in simulated discharges. The precipitation products investigated are TRMM3B42, TRMM3B42RT, GLDAS/Noah (GLDAS_Noah025SUBP_3H), APHRODITE, PERSIANN and GSMAP-MVK+. Two hydrological models of different complexities - a water and energy budget-based distributed hydrological model (WEB-DHM) (Wang et al., 2009a; Wang et al., 2009b; Wang et al., 2009c) and a physically-based semi-distributed hydrological model TOPMODEL (Beven and Kirkby, 1979) - were employed to investigate the influence of hydrological models on discharge simulations. The respective uncertainties from precipitation products, hydrological models and the combined uncertainties from the interactions between products and models are quantified using a global sensitivity analysis approach, i.e., the analysis of variance approach (ANOVA). A river basin with a series of 8-year data is used to demonstrate the methodology.

The paper is organized as follows. Section 2 introduces the study region, precipitation products, hydrological models and the proposed framework. Section 3 presents the statistical evaluation results. Hydrological evaluations and the implementation of the proposed framework are given in section 4. Discussion is given in section 5. Summary and conclusions are presented in section 6.

2 Materials and methodology

2.1 Biliu basin

Biliu basin (2814 km²), located in the coastal region between the China Bohai Sea and the China Huanghai Sea, covers longitudes 122.29°E to 122.92°E and latitudes 39.54°N to 40.35°N. This basin is characterized by a snow - winter dry - hot summer climate (Koppen climate classification) and the average annual temperature is 10.6°C. Summer (July to September) is the major rainy season. There are 11 rainfall stations and one discharge gauge which have historical data from January 2000 to December 2007. The average elevation is 240 meters. The gauge distribution in Biliu is shown in Fig. 1. The basin slopes vary from 0 to 38 degrees. Land-use data are obtained from the USGS (<http://edc2.usgs.gov/glcc/glcc.php>). The land-use types have been reclassified to SiB2 land-use types for this study (Sellers et al., 1996). There are six land-use types, with broadleaf and needle leaf trees and short vegetation being the main types. Soil data are obtained from the Food and Agriculture Organization (FAO) (2003) Global data product, and there are two types of soil in the basin: clay loam-luvisols and loam-phaeozems.

2.2 Precipitation products

The selected precipitation products are shown in Table 1. These data are all freely available. In these selected precipitation products, APHRODITE is wholly based on gauge data; TRMM3B42 and GLDAS are remote satellite estimation with gauge data corrections; while others are remote satellite estimation without gauge data corrections. Remote-based precipitation estimation has many weaknesses, e.g., microwave estimation could miss convective rainfall and typhoon rain because of its sparse time interval resolution; infrared

estimation has a higher time interval resolution, but it cannot penetrate thick clouds. Ground rain gauge-based interpolation products are limited by interpolation algorithms, gauge density and gauge data quality (Xie et al., 2007). The details of data sources used in each precipitation product can be found in Table 1. The detailed introductions of these products are as follows.

TRMM is a joint mission between NASA and Japan Aerospace Exploration Agency designed to monitor and study tropical rainfall (Kummerow et al., 2000; Huffman et al., 2007). Three instruments - a visible infrared radiometer, a TRMM microwave imager and a precipitation radar - are employed to obtain accurate precipitation estimation. The TRMM precipitation radar is the first space-based precipitation radar and operates between 35°N and 35°S. Outside this band, the microwave imager is used between 40°N and 40°S, and the visible infrared radiometer data are used between 50°N to 50°S. Usually the precipitation radar is considered to give the most accurate estimation from satellite, and data from it are often used for calibration of passive microwave data from other instruments (Ebert et al., 2007). The post-real-time product used in this study is the TRMM3B42, which utilizes three data sources: the TRMM combined instrument estimation using data from both TRMM precipitation radar and the microwave imager; the GPCP monthly rain gauge analysis developed by the Global Precipitation Climatology Center; and the Climate Assessment and Monitoring System monthly rain gauge analysis. TRMM3B42 applies an infrared to rain rate relationship using histogram matching, while TRMM3B42RT merges microwave and infrared precipitation estimation.

PERSIANN is a product that, using an artificial neural network function, estimates precipitation by combining infrared precipitation estimation and the TRMM combined

instrument estimation (which assimilates with TRMM precipitation radar and microwave data). GSMAP-MVK+ uses microwave and infrared precipitation data together and combines cloud motion vectors to generate fine-resolution precipitation estimation.

The Global Land Data Assimilation System (GLDAS) project is an extension of the existing and more mature North American Land Data Assimilation System (Rodell et al., 2004). It integrates satellite- and ground-based data sets for parameterizing, forcing and constraining a few offline land surface models for generating optimal fields of land surface states and fluxes. At present, GLDAS drives four Land Surface Models: Mosaic (Koster and Suarez, 1992), Noah (Chen et al., 1996; Betts et al., 1997; Koren et al., 1999; Ek, 2003), the Community Land Model (Dai et al., 2003) and Variable Infiltration Capacity model (Liang et al., 1994). Among them, the GLDAS/Noah Land Surface Model product (GLDAS_NOAH025SUBP_3H) has a 3-h $0.25^\circ \times 0.25^\circ$ resolution, which is desirable for basin scale research. The GLDAS precipitation data combine microwave and infrared, and also assimilate gauge observations.

2.3 Criteria for accuracy assessment

Uncertainties of precipitation products are evaluated on the basis of basin-averaged rainfall observations. Four evaluation criteria are used in rainfall amount error assessment: correlation coefficient (CC), root mean square error (RMSE), Nash-Sutcliffe coefficient of efficiency (NSE) and relative bias (RB). These are calculated as follows:

$$\text{RMSE} = \left(\frac{\sum_{i=1}^n (X_{pi} - X_{oi})^2}{n} \right)^{\frac{1}{2}} \quad (1)$$

$$\text{NSE} = 1 - \frac{\sum_{i=1}^n (X_{pi} - X_{oi})^2}{\sum_{i=1}^n (X_{oi} - \overline{X_o})^2} \quad (2)$$

$$\text{RB} = \frac{\sum_{i=1}^n X_{pi} - \sum_{i=1}^n X_{oi}}{\sum_{i=1}^n X_{oi}} \times 100\% \quad (3)$$

where X_{oi} represents observed data; X_{pi} represents estimated data; n is the total number of data points. A perfect fit should have CC and NSE values of one. The lower the RMSE and RB, the better the estimation. These comparison criteria have been used by many studies (Ebert et al., 2007; Wang et al., 2011; Yong et al., 2012), so they are used in this study.

Probability distributions by occurrence and volume are also analyzed, which can provide us with the information on the frequency and on the product error dependence on precipitation intensity (Chen et al., 2013a; Chen et al., 2013b). The critical success index (CSI), probability of detection (POD) and false alarm ratio (FAR) are used to quantify the ability of precipitation products to detect observed rainfall events. These are defined as follows:

$$\text{CSI} = \frac{H}{H + M + F} \quad (4)$$

$$\text{POD} = \frac{H}{H + M} \quad (5)$$

$$\text{FAR} = \frac{F}{H + F} \quad (6)$$

where H is the total number of hits; M is the total number of misses; F is the total number of false alarms (Ebert et al., 2007; Su et al., 2008). A perfect detection should have CSI and POD values equal to one and a FAR value of zero.

2.4 Hydrological models and data

2.4.1 WEB-DHM

The distributed biosphere hydrological model, WEB-DHM (Wang et al., 2009a;Wang et al., 2009b;Wang et al., 2009c), was developed by coupling a simple biosphere scheme (Sellers et al., 1986) with a geomorphology-based hydrological model (Yang, 1998) to describe water, energy and CO_2 fluxes at a basin scale. WEB-DHM has been used in several evaluations and applications (Wang et al., 2010a;Wang et al., 2010b;Wang et al., 2012;Shrestha et al., 2013).

WEB-DHM input data include precipitation, temperature, downward solar radiation, long wave radiation, air pressure, wind speed and humidity. With the exception of precipitation, all input data are obtained from automatic weather stations. There are three automatic weather stations near Biliu, and observations from these are obtained from the China Meteorological Data Sharing Service System (downloaded from <http://cdc.cma.gov.cn/home.do>). Hourly precipitation data are downscaled from daily rain gauge observations using a stochastic method (Wang et al., 2011). Hourly temperatures are calculated from daily maximum and minimum temperatures using the TEMP model (Parton and Logan, 1981). The estimated temperatures are also further evaluated using daily average temperature. Downward solar radiation is estimated from sunshine duration, temperature and humidity using a hybrid model (Yang et al., 2006). Long wave radiation is obtained from the GLDAS/Noah (Rodell et al., 2004). Air pressure is estimated according to altitude (Yang et al., 2006). These meteorological data are then interpolated to $300\text{ m} \times 300\text{ m}$ model cells through an inverse-distance weighting approach. Because of the elevation differences among model cells and meteorological gauges, the interpolated surface air temperatures are further modified

with a lapse rate of 6.5K/km. Gauge rainfall data are also interpolated to 300 m \times 300 m model cells and basin-averaged gauge rainfall data are calculated on the basis of interpolation results. In addition to the above, the leaf area index and fraction of photosynthetically active radiation data are obtained from level-4 MODIS global products-MOD11A2. Digital Elevation Model (DEM) is from the NASA SRTM (Shuttle Radar Topographic Mission) with a resolution of 30 m \times 30 m. We resampled the resolution to 300 m in model calculation to reduce computation cost, while the model processed finer DEM (30 m grid) to generate sub-grid parameters (such as hillslope angle and length).

2.4.2 TOPMODEL

TOPMODEL is a physically-based, variable contributing area model of basin hydrology which attempts to combine the advantages of a simple lumped parameter model with distributed effects (Beven and Kirkby, 1979). Fundamental to TOPMODEL's parameterization are three assumptions: (1) saturated-zone dynamics can be approximated by successive steady-state representations; (2) hydrological gradients of the saturated zone can be approximated by the local topographic surface slope; and (3) the transmissivity profile whose form declines exponentially with increasing vertical depth of the water table or storage is spatially constant. On the basis of the above mentioned assumptions, the index of hydrological similarity is represented as the topographic index, $\ln(a / \tan \beta)$, for which a is the area per unit contour length and β is the local slope angle. More detailed descriptions of TOPMODEL and its mathematical formulation can be found in Beven et al. (1979). TOPMODEL has been popularly utilized in research across the world (Blazkova and Beven, 1997;Cameron et al., 1999;Hossain and Anagnostou, 2005;Bastola et al., 2008;Gallart et al., 2008;Bouilloud et al., 2010;Qi et al., 2013), because of its relatively simple model structure.

The input data of TOPMODEL mainly includes basin averaged precipitation and topographic data which can be estimated from DEM.

2.5 The proposed framework

Fig. 2 shows the diagrammatic flowchart of the proposed framework for quantification of uncertainty contributions to ensemble discharges simulated using precipitation products. This framework includes four parts: (a) selection of precipitation products; (b) selection of hydrological models; (c) ensemble discharge simulations using the hydrological models and precipitation products; and (d) quantification of individual and interactive contributions using the analysis of variance (ANOVA) approach including contributions from precipitation products, hydrological models and interactions between models and products. Because the spatial resolution of selected precipitation products does not correspond with WEB-DHM model cells, the following procedures were carried out for basin averaged rainfall calculations: (1) resampling 0.25° or 0.1° precipitation product grids into $300\text{ m} \times 300\text{ m}$ cells (the grid size used in WEB-DHM simulations); (2) calculating basin-averaged precipitation using 300 m precipitation product grids located within the basin boundary. Diagrammatic descriptions of these procedures are shown in Fig. 1d. Because WEB-DHM needs hourly input data, for the 3-hour resolution precipitation products, we assumed rainfall is uniformly distributed within each 3-hour period. For daily resolution products, we used the same approach as downscaling observed precipitation data. This downscaling approach may affect uncertainty in simulated discharge. However, Wang et al. (2011) have already successfully applied the downscaling approach, and showing that the influence is negligible.

The total ensemble uncertainty Y is the variance of discharges. To relate Y to the uncertainty

sources, the superscripts j and k in $Y^{j,k}$ represent a combination of precipitation product j and hydrological model k

$$Y^{j,k} = P^j + M^k + PM^{j,k} \quad (7)$$

where P represents the effect of j th precipitation product, M represents the effect of k th hydrological model, and PM represents the interaction effect. In this study, j varies from one to six, and k varies from one to two. Details of the quantification are explained in the follow sections.

2.5.1 Subsampling approach

ANOVA could underestimate variance when the sample size is small (Bosshard et al., 2013). To reduce the effect of the sample size, Bosshard et al. (2013) proposed a subsampling method, which was used in this paper. In the subsampling method, the superscript j in Eq. (7) is replaced with $\mathbf{g}(h,i)$. According to Bosshard et al. (2013), in each subsampling iteration i , data from two products should be selected out of all the six products, and thus 15 combinations can be obtained. Therefore, the superscript \mathbf{g} becomes a 2×15 matrix:

$$\mathbf{g} = \begin{pmatrix} 1 & 1 & \cdots & 1 & 2 & 2 & \cdots & 4 & 4 & 5 \\ 2 & 3 & \cdots & 6 & 3 & 4 & \cdots & 5 & 6 & 6 \end{pmatrix} \quad (8)$$

2.5.2 Uncertainty contribution decomposition

Based on the ANOVA theory (Bosshard et al., 2013), total error variance (SST) can be divided into sums of squares due to the individual effects as:

$$SST = SSA + SSB + SSI \quad (9)$$

where SSA is the error contribution of precipitation products, SSB is the error contribution of

hydrological models and SSI is the error contribution of their interactions.

The terms can be estimated using the subsampling procedure as follows:

$$SST_i = \sum_{h=1}^H \sum_{k=1}^K \left(Y^{g(h,i),k} - Y^{g(o,i),o} \right)^2 \quad (10)$$

$$SSA_i = K \cdot \sum_{h=1}^H \left(Y^{g(h,i),o} - Y^{g(o,i),o} \right)^2 \quad (11)$$

$$SSB_i = H \cdot \sum_{k=1}^K \left(Y^{g(o,i),k} - Y^{g(o,i),o} \right)^2 \quad (12)$$

$$SSI_i = \sum_{h=1}^H \sum_{k=1}^K \left(Y^{g(h,i),k} - Y^{g(h,i),o} - Y^{g(o,i),k} + Y^{g(o,i),o} \right)^2 \quad (13)$$

where symbol o indicates averaging over a particular index; H is the number of precipitation products (six in this study) and K is the number of hydrological models (two in this study).

Then the variation fraction η^2 is calculated as follows:

$$\eta_{\text{precipitation}}^2 = \frac{1}{I} \sum_{i=1}^I \frac{SSA_i}{SST_i} \quad (14)$$

$$\eta_{\text{model}}^2 = \frac{1}{I} \sum_{i=1}^I \frac{SSB_i}{SST_i} \quad (15)$$

$$\eta_{\text{interaction}}^2 = \frac{1}{I} \sum_{i=1}^I \frac{SSI_i}{SST_i} \quad (16)$$

η^2 has a value between 0 and 1, which represent 0% and 100% contributions to the overall uncertainty of simulated discharges respectively. I equals 15 in this study. As shown in Eqs. 14-16, the subsampling approach is necessary because it guarantees that every contributor has the same denominator I . This same denominator makes sure that the inter-comparison among precipitation contribution, model contribution and interaction contribution is free of influence from the sampling number of precipitation products and hydrological models.

3 Statistical evaluations

3.1 Daily and monthly scales

Comparison of precipitation product data and gauge observations at a daily scale is shown in Fig. 3. Observations are shown on the x-axis and precipitation product data are shown on the y-axis. Four criteria, RMSE, CC, NSE and RB, are also shown. GSMAP-MVK+ is the best product and PERSIANN has the poorest performance with respect to RMSE and NSE. GSMAP-MVK+ is also the best with respect to CC, while GLDAS has the poorest performance with a CC value of 0.55. With respect to RB, APHRODITE performs best and GSMAP-MVK+ the second best, while TRMM3B42RT the least best with an RB value of -38%. None of the products can outperform others in terms of all the statistical criteria. This may be due to the different limitations of satellite sensors and inverse algorithms of precipitation products. This situation shows that the selection of the best precipitation products is difficult.

TRMM3B42RT and TRMM3B42 underestimate precipitation amounts. This underestimation may be because convective rainfall always happens in summer in northeast China (Shou and Xu, 2007a, b; Yuan et al., 2010), and indicates the limitation of TRMM algorithms in high latitude regions with convective rainfall. This type of rainfall has a large rainfall amount within a short time period and, therefore, cannot be captured by microwave imager. This type of rainfall may also have a thick cloud that is impenetrable by infrared (Ebert et al., 2007). Thus microwave and infrared estimation could underestimate rainfall. Compared with TRMM3B42RT, TRMM3B42 provides an improvement in RB. This improvement may be attributed to the assimilation with gauge data and histogram matching. Compared with APHRODITE and GSMAP-MVK+, TRMM3B42 has low accuracy as represented by RB.

This implies that the retrieval algorithm used by TRMM3B42 still needs to be improved with respect to RB. The reason why APHRODITE outperforms TRMM3B42 is that APHRODITE is a gauge-based product. GSMAP-MVK+ outperforms TRMM3B42 in terms of RB may be due to the cloud motion vectors it uses. Compared with GSMAP-MVK+, GLDAS/Noah precipitation shows low accuracy in all the criteria even though they use similar data sources: IR and MW.

Comparison of precipitation product data and gauge observations at a monthly scale is shown in Fig. 4. Here, the APHRODITE product (Fig. 4d) performs best based on RMSE, CC, NSE and RB. GLDAS/Noah is the poorest in terms of RMSE and NSE. With respect to CC, GLDAS and TRMM3B42 are equally poor, with CC values of 0.81. The results also show that PERSIANN overestimates precipitation amount, while Li et al. (2013) found PERSIANN underestimates rainfall in south China. This may be attributed to the different latitudes of the study regions.

Fig. 5 shows time series of average monthly precipitation data against gauge observations during the period 2000-2007. Each curve represents a different precipitation product. GLDAS data (Fig. 5a) seriously underestimate high rainfall. Similarly, TRMM3B42RT underestimates peak precipitation intensity also. Comparatively, APHRODITE, PERSIANN, TRMM3B42 and GSMAP-MVK+ have better performances.

3.2 Inter-annual evaluations

Fig. 6 shows the inter-annual average monthly precipitation. Each curve represents a different product data. PERSIANN overestimates in all the 12 months, while others underestimate,

especially during the summer. This may result from the artificial neural network function and limitations of infrared and microwave estimation. APHRODITE data are relatively close to observations. Compared with TRMM3B42RT, TRMM3B42 is better, which indicates the gauge corrections and histogram matching used by TRMM3B42 impact positively on accuracy. During the summer, discrepancies between products become larger. With a decrease of rainfall magnitude, the discrepancies between products reduce. This information implies that the differences in precipitation estimation algorithms are related to precipitation magnitudes: the larger the rainfall magnitudes, the greater the differences.

3.3 Probability distribution evaluations

Fig. 7 shows cumulative probability distribution functions (CDF) by occurrence (CDF_c) and by volume (CDF_v) for precipitation products. Probabilities are shown on the y axis, and the x axis shows rainfall intensity with a 1 mm/day interval log space.

PERSIANN is the best by both occurrence and volume. However, for CDF_c, TRMM3B42RT is the least best, and, for CDF_v, TRMM3B42RT and GLDAS/Noah are comparable and worse than others. All precipitation products overestimate occurrence and volume probabilities except rainfall intensities of larger than 63mm/day and 53mm/day for occurrence and volume probabilities, respectively. This may be because the precipitation products overestimate the intensity of some heavy rainfall (recall the results in section 3.1). The results differ from those of Li et al. (2013), in which PERSIANN has the poorest performance. This may result from differences in study region (in the study of Li et al. (2013), south China was studied).

3.4 Contingency statistics

Fig. 8 shows the false alarm ratio, probability of detection and critical success index for each precipitation product.

PERSIANN has the highest false alarm ratio among the products, while TRMM3B42RT has the lowest. The false alarm ratio of TRMM3B42 is larger than TRMM3B42RT, which indicates that the gauge corrections and histogram matching used by TRMM3B42 do not provide positive effects on false alarm ratio and may give rise to uncertainty in false alarm ratio. GSMAP-MVK+ has a lower false alarm ratio than TRMM3B42.

No obvious trends are observed for the false alarm ratio overall (compared with the probability of detection and critical success index), which means the false alarm ratio dependence on rainfall magnitude is weak. However, Chen et al. (2013a) found the false alarm ratios of TRMM3B42 and TRMM3B42RT to increase with an increase in rainfall intensity. The differences are attributed mainly to observed data. In the study of Chen et al. (2013a), national rain gauge data were employed, whereas in this study more detailed basin data are used.

Among all selected products, GLDAS/Noah has the lowest probability of detection and critical success index during periods of high rainfall intensity, while APHRODITE retains a high probability of detection and critical success index. This is because APHRODITE uses gauge observations, and implies that the APHRODITE algorithm is effective. PERSIANN has comparable probability of detection with APHRODITE. The critical success index of GSMAP-MVK+ is also comparable with APHRODITE. Compared with TRMM3B42RT,

TRMM3B42 has greater probability of detection and comparable critical success index. This information implies that retrieval algorithm of TRMM3B42 provides positive effects on probability of detection, but no obvious positive impacts on critical success index.

Decreasing trends are observed for all products in terms of probability of detection and critical success index, matching the results of Chen et al. (2013a) for TRMM3B42 and TRMM3B42RT. This indicates that probability of detection and critical success index have relatively strong dependence on rainfall magnitude, and implies microwave and infrared precipitation estimation may have relatively strong dependence on rainfall magnitude in terms of probability of detection and critical success index.

4 Hydrological evaluations

4.1 Assessment of hydrological models

WEB-DHM was calibrated against observed discharges of Biliu. Six main parameters were selected to calibrate using a trial and error approach due to the model's computational burden. Model parameter multipliers were calibrated, similar to the study by Wang et al. (2011). The 'Trial and error' approach has two steps. First, all the multiplier values are set to 1 which represents the default parameter values from Food and Agriculture Organization (FAO) (2003) and SiB2 model. Second, varying the multiplier values until acceptable discharge simulation accuracy is obtained. The calibrated parameter values are listed in Table 2. The simulated daily, monthly and inter-annual results are shown in Figs. 9a, 9c and 9e.

TOPMODEL uses basin-averaged parameter values, and these parameter values are estimated by experience or observation. However, these methods do not give precise parameter values. Therefore, the parameter values are considered as uncertain and provided with ranges based on experience (Beven and Kirkby, 1979; Beven and Freer, 2001a, b; Peters et al., 2003). Six

parameters of TOPMODEL were calibrated using the dynamically dimensioned search algorithm (Tolson and Shoemaker, 2007), and the results are given in Table 3. The simulated daily, monthly and inter-annual results are shown in Figs. 9b, 9d and 9f.

Note that the parameters of TOPMODEL and WEB-DHM were calibrated using observed precipitation data, and the accuracy of simulated discharges was validated using gauge observations. Comparison with the rainfall-runoff model parameter values reported for the case study catchment in previous research shows the parameter values are appropriate. (Qi et al., 2013; Qi et al., 2015, 2016).

4.2 Daily scale discharges

Figs. 10 and 11 display scatterplots of discharges during the period 2000-2007 simulated using WEB-DHM and TOPMODEL against gauge observations at a daily scale. Two criteria, NSE and RB, are shown. It should be noted that the start dates are different for precipitation products, and observed data were used when product data are not available: from 1 January 2000 to 29 February 2000 for TRMM3B42RT, GSMAP-MVK+ and PERSIANN; from 1 January 2000 to 23 February 2000 for GLDAS/Noah. These time periods were not considered for accuracy comparison.

In the case of WEB-DHM simulations, the best NSE (0.41) corresponds with APHRODITE (Fig. 10d), while the best value for RB (1%) corresponds with GLDAS/Noah. In the case of TOPMODEL simulations, the best NSE (0.41) corresponds with APHRODITE, and the best value for RB (-24%) corresponds with APHRODITE also. Although the best NSE is the same for both WEB-DHM and TOPMODEL simulations and corresponding product is also the

same, there is a large difference in the best RB values. At the daily scale precipitation amount evaluation, the least best RB is -38%, corresponding with TRMM3B42RT (Fig. 3c). However, in WEB-DHM discharge simulation, the least best RB (218%) corresponds with PERSIANN, and, in TOPMODEL simulation, the least best RB (-62%) corresponds with TRMM3B42RT. These differences stem from differences in hydrological models and interactions between hydrological models and precipitation product data.

All RB criteria at the daily scale precipitation evaluations (recall the results in Fig. 3) are amplified by TOPMODEL, while in the case of WEB-DHM, some are amplified and the others are decreased. For example, for GLDAS and PERSIANN, the RB criteria at the daily scale precipitation evaluations are -27% and 28%, but they are -50% and 31% in TOPMODEL simulations; they are 1% and 218% in WEB-DHM simulations. These differences result from the influence of hydrological models and interactions between precipitation products and hydrological models. These results reveal that a hydrological model can amplify uncertainties in input data but also reduce uncertainties, which may be due to the nonlinear runoff generation process in hydrological models. This finding is consistent with the research by Yong et al. (2010).

4.3 Monthly scale discharges

Figs. 12 and 13 display scatterplots of discharges during the period 2000-2007 simulated using WEB-DHM and TOPMODEL against gauge observations at a monthly scale.

In the case of WEB-DHM, the best NSE and RB values are 0.73 and 1%, which corresponding with TRMM3B42 and GLDAS respectively. In the case of TOPMODEL, they

are 0.58 and -24%, corresponding with PERSIANN and APHRODITE respectively. The combination of WEB-DHM and TRMM3B42 shows a satisfactory performance, with NSE and RB values of up to 0.73 and -7%, even though TRMM3B42 is not the best in monthly scale precipitation data evaluation. This reveals the influence of different combinations of hydrological models and precipitation data on discharge simulation, implying that accurate discharge simulation does not solely depend on the accuracy of a precipitation product.

At the monthly scale, although APHRODITE is the best precipitation product and WEB-DHM model has better performance than TOPMODEL in calibration (Figs. 9c and 9d), the combination of APHRODITE and WEB-DHM is not better in the discharge simulation, which can be shown by comparing Fig. 12d with Fig. 13d (the RB and NSE of WEB-DHM and APHRODITE combination are -37% and 0.5, but they are -24% and 0.51 for the combination of TOPMODEL and APHRODITE). This could be due to the interactive influence between hydrological models and precipitation products, and implies that the interactions between models and products could be large and have a big influence on discharge simulations. In addition, comparison of Figs. 12d and 12b shows that discharge simulation of APHRODITE is worse than TRMM3B42, even though APHRODITE is the best precipitation product in terms of all the selected criteria at a monthly scale precipitation amount evaluation. This information shows that better precipitation products do not guarantee better discharge simulations. These results imply that, although the satellite-based precipitation products are not as accurate as gauge-based products in rainfall amount estimation, they could have a better performance in discharge simulations if the combination of precipitation product and hydrological model is good.

4.4 Inter-annual average monthly discharges

Fig. 14 shows inter-annual average monthly discharges of all selected precipitation products during the period 2000-2007. In the case of TOPMODEL, PERSIANN agrees well with gauge observations, and all products underestimate discharges in August. In the case of WEB-DHM, GLDAS data and TRMM3B42 data have a better performance than other data but, with the exception of PERSIANN, all products underestimate peak discharge in August. The simulation results show huge differences even though Figs. 9e and 9f show TOPMODEL and WEB-DHM have almost the same performance using observed data; this is because of the impacts of interactive influence between hydrological models and precipitation products.

4.5 Uncertainty source quantification

All above results suggest that discharge simulations are influenced by precipitation products, hydrological models and interactions between hydrological models and precipitation products. Thus it is essential to quantify the respective influence. Figs. 15a and 15b show contributions of precipitation products, hydrological models and their interactions to uncertainties in monthly average discharges and different flow quantiles respectively. Fig. 15b shows quantiles computed at a daily time step. The contributions of uncertainty sources are represented by stripes.

Fig. 15a shows that precipitation data contribute most of the uncertainty in discharges, and contribute more than hydrological models. Interactions between hydrological models and precipitation products have large contributions, at a similar level to those from hydrological models. In summer (July to September), the contribution of precipitation data is less than

most other months except March. However, the uncertainty in precipitation intensity increases in summer (recall the results in section 3.2). In non-summer months except March, the uncertainty contribution from precipitation products is larger than in summer. These differences maybe result from the nonlinear propagation of uncertainty through hydrological models. In March, the contribution of hydrological models is larger than in other months, which may result from the decrease in influences of interactions and precipitation products, and from the nonlinear influence of the hydrological models.

Fig. 15b shows that, for small discharges (smaller than 25% quantile which corresponds to an observed discharge value of $1.79\text{m}^3/\text{s}$) and large discharges (larger than 99% quantile which corresponds to an observed discharge value of $157\text{m}^3/\text{s}$), hydrological models contribute most of the uncertainties. For middle magnitude flows (between 25% and 99% quantiles), precipitation products contribute the majority, and the contribution of interactions is not negligible and of similar magnitude to the contribution from hydrological models. The contribution of interactions is larger for middle magnitude flows than for small and large discharges. The different contributions of interactions for various magnitude flows may be because different magnitude rainfall data could trigger different hydrological processes (Herman et al., 2013). Small discharges mainly come from base flows which are relatively stable and do not need much rainfall to be triggered, and large discharges are mainly controlled by overland flows when heavy precipitation occurs. Middle magnitude discharges consist of contributions from base flows, lateral subsurface flows and overland flows, ~~and, It is more complex and~~ can be triggered by rainfalls of various magnitudes ~~rainfalls~~ thus interactions are more variable~~changeable~~.

Although heavy rainfall data have high uncertainty (recall the results in section 3.1),

precipitation products have a small contribution to uncertainty in large discharges (Fig. 15b). This implies that the uncertainty in high precipitation is compensated by the high nonlinearity in hydrological models.

In this study, because hydrological model parameters were calibrated using gauge observations, the hydrological model parameter uncertainty was not considered. Although the uncertainty contribution results in this study may not be transferable to other basins, the proposed framework provides a useful tool for quantifying uncertainty contributions in discharge simulations using precipitation products.

5 Discussion

The spatial variations in precipitation are not considered in this study. The study region is a small river basin, as shown in Fig. 1, there are only 11 grids inside the basin boundary for the precipitation products with a spatial resolution of 0.25 degree. Within a grid of 0.25 degree, there are no differences in precipitation amount between the 300 m \times 300 m grids used in hydrological models, and differences exist at the level of 0.25 degree grids only. Sapriza-Azuri et al. (2015) suggested that the spatial variability of precipitation has little influence on rapidly responding river discharges; this study is the case because the flow transport time from the most upper part of the basin to the downstream discharge gauge is 6 hours, which is shorter than the daily and monthly time steps of discharges investigated. Therefore, the spatial distributions of precipitation products with a resolution of 0.25 degree in the relatively small river basin have little influence on the simulated discharges. However, the assumption of uniform distribution can be regarded as another uncertainty source against spatial variability, and its influence can be assessed using the proposed uncertainty quantification framework. This will allow us to compare the relative contributions of the

assumption to those from other sources such as hydrological models, which will be investigated using a much larger river basin in ~~the~~ future work.

In addition to improving the accuracy of precipitation products, a good ~~coalition~~ ~~eollation~~ could help to achieve the performance in discharge simulations. Our approach provides a way to assess the different coalitions, i.e., the overall uncertainties in simulated discharges from different combinations of hydrological models and precipitation products. More precipitation products and hydrological models should be included and tested in ~~the~~ future work.

It should be noted that other input data including temperature, downward solar radiation, long wave radiation, air pressure, wind speed and humidity may also have uncertainties. However, Fig. 9 shows that the simulated discharge data are acceptable particularly at monthly and inter-annual scales using these data. Research has shown that the land surface temperatures are highly accurate compared with MODIS satellite land surface temperature observations (Wang et al., 2011; Qi et al., 2015). Thus, the uncertainties from the other inputs are not considered in our case study river basin.

In this study, the parameter values calibrated using gauge observations are not tuned to a specific product. That is, there is little compensation ~~by~~ model parameters for the errors in input precipitation data. The differences in model~~ing~~ accuracy mainly results from the different representations of hydrological processes. That is, the errors in precipitation products are primarily compensated by the different representations of model processes.

6 Summary and conclusions

This research assesses the applicability of six precipitation products with fine spatial and temporal resolutions at a high latitude region in northeast China using both statistical and hydrological evaluation methods at multi-temporal scales. A framework is proposed to quantify uncertainty contributions of precipitation products, hydrological models and their interactions to simulated discharges. These products are TRMM version 7 products (TRMM3B42 and TRMM3B42RT), GLDAS, APHRODITE, PERSIANN and GSMAP-MVK+. The fully distributed WEB-DHM and semi-distributed TOPMODEL were employed to investigate the influence of hydrological models on simulated discharges. The results show the uncertainty characteristics of the six products, and reveal strategies that could improve precipitation products. This information could ~~be able to~~ provide references for future precipitation product development. The proposed framework can reveal hydrological simulation uncertainties using precipitation products: thus provides useful information on precipitation product applications. The following conclusions are presented on the basis of this study.

First, at daily scale, selecting the best precipitation products is very difficult, while, at a monthly scale, APHRODITE has the best performance in terms of NSE, RB, RMSE, and CC, and also retains a high probability of detection and critical success index. This information implies that the APHRODITE algorithm is effective, and APHRODITE could be a very good data set to refine and validate satellite-based precipitation products.

Second, GSMAP-MVK+ show huge advantage, and is better than TRMM3B42 in RB, NSE, RMSE, CC, false alarm ratio and critical success index, while PERSIANN is better than TRMM3B42 in probability of detection and precipitation probability distribution estimation.

At present, the ~~new precipitation estimation mission~~—NASA Global Precipitation

Measurement (GPM) [mission](#) combines the artificial neural network function of PERSIANN and precipitation radar-matching of TRMM Multi-satellite Precipitation Analysis. However, the above finding implies that incorporating GSMAP-MVK+ estimation approach into GPM could be useful as well.

Third, it is found that, although high uncertainty exists in heavy rainfall, hydrological models contribute mostly to the uncertainty in extreme discharges. This may result from the nonlinear propagation of uncertainty through hydrological models enlarges the influence of hydrological models, and implies that high uncertainties in extreme rainfall do not mean high uncertainties in extreme discharges.

Fourth, interactions between hydrological models and precipitation products contribute a lot to uncertainty in discharge simulations, and interactive impacts are influenced by discharge magnitude. Because of interactive effects, for hydrological models with similar performances in calibration, using the same precipitation products for discharge simulations does not provide a similar level of accuracy in discharge simulations, and in fact very different predictions could be obtained. In addition, this finding implies that only considering precipitation products or hydrological model uncertainties could result in overestimation of precipitation product contribution and hydrological model contribution to discharge uncertainty.

Fifth, a good discharge simulation depends on a good coalition of a hydrological model and a precipitation product, and a better precipitation product does not necessarily guarantee a better discharge simulation. This suggests that, although the satellite-based precipitation products are not as accurate as the gauge-based product, they could have better performance

in discharge simulations when appropriately combined with hydrological models. It should be noted that this finding should be further tested with more river basins, in particular large river basins accounting for spatial variability in precipitation products.

In the future, calculating deterministic discharge simulations considering precipitation product uncertainties and hydrological model uncertainties together should be studied because above results show product uncertainties and model uncertainties all are important. In addition, recalibrating hydrological models using precipitation products may reduce the interactive influence between hydrological models and precipitation products on simulated discharges, and this may explain why recalibration can improve discharge simulation accuracy. This should be verified in future work. Further, future research is encouraged to incorporate GSMAP-MVK+ estimation approach into GPM because of the good performance of GSMAP-MVK+.

Acknowledgements:

This study was supported by the National Natural Science Foundation of China (Grant No. 51320105010 and 51279021). The first author gratefully acknowledges the financial support provided by the China Scholarship Council. The APHRODITE data were downloaded from <http://www.chikyu.ac.jp/precip/products/index.html>. The TRMM 3B42 data are downloaded from <http://mirador.gsfc.nasa.gov/cgi-bin/mirador/presentNavigation.pl?tree=project&project=TRMM&dataGroup=Gridded>. TRMM 3B40RT data are downloaded from <ftp://trmmopen.nascom.nasa.gov/pub/merged/combinedMicro/>. TRMM 3B41RT data are downloaded from <ftp://trmmopen.nascom.nasa.gov/pub/merged/calibratedIR/>. TRMM3B42RT data are downloaded from <ftp://trmmopen.nascom.nasa.gov/pub/merged/mer>

geIRMicro/. PERSIANN data are downloaded from <http://chrs.web.uci.edu/persiann/data.html>. GSMAP_MVK data are downloaded from http://sharaku.eorc.jaxa.jp/GSMaP_crest/. The GLDAS data are downloaded from http://mirador.gsfc.nasa.gov/cgi-bin/mirador/homepageAlt.pl?keyword=GLDAS_NOAH025SUBP_3H. The data of Biliu basin were obtained from the Biliu reservoir administration.

References

- Aonashi, K., Awaka, J., Hirose, M., Kozu, T., Kubota, T., Liu, G., Shige, S., Kida, S., Seto, S., Takahashi, N., and Takayabu, Y. N.: GSMaP Passive Microwave Precipitation Retrieval Algorithm: Algorithm Description and Validation, *Journal of the Meteorological Society of Japan*, 87A, 119-136, 10.2151/jmsj.87A.119, 2009.
- Artan, G., Gadain, H., Smith, J. L., Asante, K., Bandaragoda, C. J., and Verdin, J. P.: Adequacy of satellite derived rainfall data for stream flow modeling, *Natural Hazards*, 43, 167-185, 10.1007/s11069-007-9121-6, 2007.
- Asadullah, A., McIntyre, N., and Kigobe, M. A. X.: Evaluation of five satellite products for estimation of rainfall over Uganda, *Hydrological Sciences Journal*, 53, 1137-1150, 10.1623/hysj.53.6.1137, 2008.
- Bastola, S., Ishidaira, H., and Takeuchi, K.: Regionalisation of hydrological model parameters under parameter uncertainty: A case study involving TOPMODEL and basins across the globe, *Journal of Hydrology*, 357, 188-206, 10.1016/j.jhydrol.2008.05.007, 2008.

731 Betts, A. K., Chen, F., Mitchell, K. E., and Janjic, Z. I.: Assessment of the land surface and
 732 boundary layer models in two operational versions of the NCEP Eta Model using FIFE
 733 data, Monthly Weather Review, 125, 2896-2916,
 734 10.1175/1520-0493(1997)125<2896:aotlsa>2.0.co;2, 1997.

735 Beven, K. J., and Binley, A.: The future of distributed models: model calibration and
 736 uncertainty prediction, Hydrological Processes, 6, 279-298, 10.1002/hyp.3360060305,
 737 1992.

738 Beven, K. J., and Freer, J. E.: A dynamic TOPMODEL, Hydrological Processes, 15,
 739 1993-2011, 10.1002/hyp.252, 2001a.

740 Beven, K. J., and Freer, J. E.: Equifinality, data assimilation, and uncertainty estimation in
 741 mechanistic modelling of complex environmental systems using the GLUE methodology,
 742 Journal of Hydrology, 249, 11–29, 10.1016/S0022-1694(01)00421-8, 2001b.

743 Beven, K. J., and Kirkby, M. J.: A physically based, variable contributing area model of basin
 744 hydrology, Hydrological Sciences Bulletin, 24, 43-69, 10.1080/02626667909491834,
 745 1979.

746 Blasone, R.-S., Vrugt, J. A., Madsen, H., Rosbjerg, D., Robinson, B. A., and Zyvoloski, G. A.:
 747 Generalized likelihood uncertainty estimation (GLUE) using adaptive Markov Chain
 748 Monte Carlo sampling, Advances in Water Resources, 31, 630-648,
 749 10.1016/j.advwatres.2007.12.003, 2008.

750 Blazkova, S., and Beven, K.: Flood frequency prediction for data limited catchments in the
 751 Czech Republic using a stochastic rainfall model and TOPMODEL, Journal of Hydrology,

195, 256-278, 10.1016/S0022-1694(96)03238-6, 1997.

Bosshard, T., Carambia, M., Goergen, K., Kotlarski, S., Krahe, P., Zappa, M., and Schär, C.: Quantifying uncertainty sources in an ensemble of hydrological climate-impact projections, *Water Resources Research*, 49, 1523-1536, 10.1029/2011wr011533, 2013.

Bouilloud, L., Chancibault, K., Vincendon, B., Ducrocq, V., Habets, F., Saulnier, G.-M., Anquetin, S., Martin, E., and Noilhan, J.: Coupling the ISBA Land Surface Model and the TOPMODEL Hydrological Model for Mediterranean Flash-Flood Forecasting: Description, Calibration, and Validation, *Journal of Hydrometeorology*, 11, 315-333, 10.1175/2009jhm1163.1, 2010.

Buarque, D. C., de Paiva, R. C. D., Clarke, R. T., and Mendes, C. A. B.: A comparison of Amazon rainfall characteristics derived from TRMM, CMORPH and the Brazilian national rain gauge network, *Journal of Geophysical Research*, 116, 10.1029/2011jd016060, 2011.

Cameron, D. S., Beven, K. J., Tawn, J., Blazkova, S., and Naden, P.: Flood frequency estimation by continuous simulation for a gauged upland catchment (with uncertainty), *Journal of Hydrology*, 219, 169-187, 10.1016/S0022-1694(99)00057-8, 1999.

Chen, F., Mitchell, K., Schaake, J., Xue, Y., Pan, H.-L., Koren, V., Duan, Q. Y., Ek, M., and Betts, A.: Modeling of land surface evaporation by four schemes and comparison with FIFE observations, *Journal of Geophysical Research*, 101, 7251, 10.1029/95jd02165, 1996.

Chen, S., Hong, Y., Cao, Q., Gourley, J. J., Kirstetter, P.-E., Yong, B., Tian, Y., Zhang, Z.,

773 Shen, Y., Hu, J., and Hardy, J.: Similarity and difference of the two successive V6 and V7
774 TRMM multisatellite precipitation analysis performance over China, *Journal of*
775 *Geophysical Research: Atmospheres*, 118, 13,060-013,074, 10.1002/2013jd019964,
776 2013a.

777 Chen, S., Hong, Y., Gourley, J. J., Huffman, G. J., Tian, Y., Cao, Q., Yong, B., Kirstetter, P.-E.,
778 Hu, J., Hardy, J., Li, Z., Khan, S. I., and Xue, X.: Evaluation of the successive V6 and V7
779 TRMM multisatellite precipitation analysis over the Continental United States, *Water*
780 *Resources Research*, 49, 8174-8186, 10.1002/2012wr012795, 2013b.

781 Dai, Y., Zeng, X., Dickinson, R. E., Baker, I., Bonan, G. B., Bosilovich, M. G., Denning, A.
782 S., Dirmeyer, P. A., Houser, P. R., Niu, G., Oleson, K. W., Schlosser, C. A., and Yang,
783 Z.-L.: The Common Land Model, *Bulletin of the American Meteorological Society*, 84,
784 1013-1023, 10.1175/bams-84-8-1013, 2003.

785 Dinku, T., Connor, S. J., Ceccato, P., and Ropelewski, C. F.: Comparison of global gridded
786 precipitation products over a mountainous region of Africa, *International Journal of*
787 *Climatology*, 28, 1627-1638, 10.1002/joc.1669, 2008.

788 Ebert, E. E., Janowiak, J. E., and Kidd, C.: Comparison of Near-Real-Time Precipitation
789 Estimates from Satellite Observations and Numerical Models, *Bulletin of the American*
790 *Meteorological Society*, 88, 47-64, 10.1175/bams-88-1-47, 2007.

791 Ek, M. B.: Implementation of Noah land surface model advances in the National Centers for
792 Environmental Prediction operational mesoscale Eta model, *Journal of Geophysical*
793 *Research*, 108, 10.1029/2002jd003296, 2003.

794 Freer, J. E., Beven, K. J., and Ambroise, B.: Bayesian Estimation of Uncertainty in Runoff
795 Prediction and the Value of Data: An Application of the GLUE Approach, *Water*
796 *Resources Research*, 32, 2161-2173, 10.1029/95wr03723, 1996.

797 Gallart, F., Latron, J., Llorens, P., and Beven, K. J.: Upscaling discrete internal observations
798 for obtaining catchment-averaged TOPMODEL parameters in a small Mediterranean
799 mountain basin, *Physics and Chemistry of the Earth*, 33, 1090-1094,
800 10.1016/j.pce.2008.03.003, 2008.

801 Gao, Y. C., and Liu, M. F.: Evaluation of high-resolution satellite precipitation products using
802 rain gauge observations over the Tibetan Plateau, *Hydrology and Earth System Sciences*,
803 17, 837-849, 10.5194/hess-17-837-2013, 2013.

804 Heidari, A., Saghaian, B., and Maknoon, R.: Assessment of flood forecasting lead time based
805 on generalized likelihood uncertainty estimation approach, *Stochastic Environmental*
806 *Research and Risk Assessment*, 20, 363-380, 10.1007/s00477-006-0032-y, 2006.

807 Herman, J. D., Reed, P. M., and Wagener, T.: Time - varying sensitivity analysis clarifies the
808 effects of watershed model formulation on model behavior, *Water Resources Research*,
809 49, 1400-1414, 10.1002/wrcr.20124, 2013.

810 Hong, Y., Hsu, K.-l., Moradkhani, H., and Sorooshian, S.: Uncertainty quantification of
811 satellite precipitation estimation and Monte Carlo assessment of the error propagation
812 into hydrologic response, *Water Resources Research*, 42, 10.1029/2005wr004398, 2006.

813 Hossain, F., and Anagnostou, E. N.: Assessment of a stochastic interpolation based parameter
814 sampling scheme for efficient uncertainty analyses of hydrologic models, *Computers &*

815 Geosciences, 31, 497-512, 10.1016/j.cageo.2004.11.001, 2005.

816 Huffman, G. J., Bolvin, D. T., Nelkin, E. J., Wolff, D. B., Adler, R. F., Gu, G., Hong, Y.,
817 Bowman, K. P., and Stocker, E. F.: The TRMM Multisatellite Precipitation Analysis
818 (TMPA): Quasi-Global, Multiyear, Combined-Sensor Precipitation Estimates at Fine
819 Scales, *Journal of Hydrometeorology*, 8, 38-55, 10.1175/jhm560.1, 2007.

820 Jiang, S., Ren, L., Hong, Y., Yong, B., Yang, X., Yuan, F., and Ma, M.: Comprehensive
821 evaluation of multi-satellite precipitation products with a dense rain gauge network and
822 optimally merging their simulated hydrological flows using the Bayesian model
823 averaging method, *Journal of Hydrology*, 452-453, 213-225,
824 10.1016/j.jhydrol.2012.05.055, 2012.

825 Kato, H., Rodell, M., Beyrich, F., Cleugh, H., Gorsel, E. v., Liu, H., and Meyers, T. P.:
826 Sensitivity of Land Surface Simulations to Model Physics, Land Characteristics, and
827 Forcings, at Four CEOP Sites, *Journal of the Meteorological Society of Japan*, 85A,
828 187-204, 10.2151/jmsj.85A.187, 2007.

829 Kneis, D., Chatterjee, C., and Singh, R.: Evaluation of TRMM rainfall estimates over a large
830 Indian river basin (Mahanadi), *Hydrology and Earth System Sciences*, 18, 2493-2502,
831 10.5194/hess-18-2493-2014, 2014.

832 Koren, V., Schaake, J., Mitchell, K., Duan, Q. Y., Chen, F., and Baker, J. M.: A
833 parameterization of snowpack and frozen ground intended for NCEP weather and climate
834 models, *Journal of Geophysical Research*, 104, 19569, 10.1029/1999jd900232, 1999.

835 Koster, R. D., and Suarez, M. J.: Modeling the land surface boundary in climate models as a

836 composite of independent vegetation stands, *Journal of Geophysical*
837 *Research-Atmospheres*, 97, 2697-2715, 10.1029/91JD01696, 1992.

838 Kubota, T., Shige, S., Hashizume, H., Aonashi, K., Takahashi, N., Seto, S., Hirose, M.,
839 Takayabu, Y. N., Ushio, T., Nakagawa, K., Wanami, K., Kachi, M., and Okamoto, K.:
840 Global precipitation map using satellite-borne microwave radiometers by the GSMap
841 project: Production and validation, *IEEE Transactions on Geoscience and Remote*
842 *Sensing*, 45, 2259-2275, 10.1109/tgrs.2007.895337, 2007.

843 Kuczera, G., Kavetski, D., Franks, S., and Thyer, M.: Towards a Bayesian total error analysis
844 of conceptual rainfall-runoff models: Characterising model error using storm-dependent
845 parameters, *Journal of Hydrology*, 331, 161-177, 10.1016/j.jhydrol.2006.05.010, 2006.

846 Kuczera, G., and Parent, E.: Monte Carlo assessment of parameter uncertainty in conceptual
847 catchment models- the Metropolis algorithm, *Journal of Hydrology*, 211, 69-85,
848 10.1016/S0022-1694(98)00198-X, 1998.

849 Kummerow, C., Simpson, J., and Thiele, O.: The status of the Tropical Rainfall Measuring
850 Mission (TRMM) after two years in orbit, *Journal of Applied Meteorology and*
851 *Climatology* 39, 10.1175/1520-0450(2001)040<1965:TSOTTR>2.0.CO;2, 2000.

852 Li, Z., Yang, D., and Hong, Y.: Multi-scale evaluation of high-resolution multi-sensor blended
853 global precipitation products over the Yangtze River, *Journal of Hydrology*, 500, 157-169,
854 10.1016/j.jhydrol.2013.07.023, 2013.

855 Liang, X., Lettenmaier, D. P., Wood, E. F., and Burges, S. J.: A simple hydrologically based
856 model of land-surface water and energy fluxes for general-circulation models, *Journal of*

857 Geophysical Research-Atmospheres, 99, 14415-14428, 10.1029/94jd00483, 1994.

858 Müller, M. F., and Thompson, S. E.: Bias adjustment of satellite rainfall data through
859 stochastic modeling: Methods development and application to Nepal, *Advances in Water*
860 *Resources*, 60, 121-134, 10.1016/j.advwatres.2013.08.004, 2013.

861 Maggioni, V., Vergara, H. J., Anagnostou, E. N., Gourley, J. J., Hong, Y., and Stampoulis, D.:
862 Investigating the Applicability of Error Correction Ensembles of Satellite Rainfall
863 Products in River Flow Simulations, *Journal of Hydrometeorology*, 14, 1194-1211,
864 10.1175/jhm-d-12-074.1, 2013.

865 Meng, J., Li, L., Hao, Z., Wang, J., and Shao, Q.: Suitability of TRMM satellite rainfall in
866 driving a distributed hydrological model in the source region of Yellow River, *Journal of*
867 *Hydrology*, 509, 320-332, 10.1016/j.jhydrol.2013.11.049, 2014.

868 Nikolopoulos, E. I., Anagnostou, E. N., Hossain, F., Gebremichael, M., and Borga, M.:
869 Understanding the Scale Relationships of Uncertainty Propagation of Satellite Rainfall
870 through a Distributed Hydrologic Model, *Journal of Hydrometeorology*, 11, 520-532,
871 10.1175/2009jhm1169.1, 2010.

872 Ochoa, A., Pineda, L., Crespo, P., and Willems, P.: Evaluation of TRMM 3B42 precipitation
873 estimates and WRF retrospective precipitation simulation over the Pacific–Andean region
874 of Ecuador and Peru, *Hydrology and Earth System Sciences*, 18, 3179-3193,
875 10.5194/hess-18-3179-2014, 2014.

876 Pan, M., Li, H., and Wood, E.: Assessing the skill of satellite-based precipitation estimates in
877 hydrologic applications, *Water Resources Research*, 46, 10.1029/2009wr008290, 2010.

878 Parton, W. J., and Logan, J. A.: A model for diurnal variation in soil and air temperature,
879 Agricultural Meteorology, 23, 205-216, 10.1016/0002-1571(81)90105-9, 1981.

880 Peng, Z., Wang, Q. J., Bennett, J. C., Pokhrel, P., and Wang, Z.: Seasonal precipitation
881 forecasts over China using monthly large-scale oceanic-atmospheric indices, Journal of
882 Hydrology, 519, 792-802, 10.1016/j.jhydrol.2014.08.012, 2014a.

883 Peng, Z., Wang, Q. J., Bennett, J. C., Schepen, A., Pappenberger, F., Pokhrel, P., and Wang, Z.:
884 Statistical calibration and bridging of ECMWF System4 outputs for forecasting seasonal
885 precipitation over China, Journal of Geophysical Research: Atmospheres, 119, 7116-7135,
886 10.1002/2013jd021162, 2014b.

887 Peters, N. E., Freer, J., and Beven, K.: Modelling hydrologic responses in a small forested
888 catchment (Panola Mountain, Georgia, USA): a comparison of the original and a new
889 dynamic TOPMODEL, Hydrological Processes, 17, 345-362, 10.1002/hyp.1128, 2003.

890 Qi, W., Zhang, C., Chu, J., and Zhou, H.: Sobol's sensitivity analysis for TOPMODEL
891 hydrological model: A case study for the Biliu River Basin, China, Journal of Hydrology
892 and Environment Research, 1, 1-10, 2013.

893 Qi, W., Zhang, C., Fu, G., and Zhou, H.: Global Land Data Assimilation System data
894 assessment using a distributed biosphere hydrological model, Journal of Hydrology, 528,
895 652-667, 10.1016/j.jhydrol.2015.07.011, 2015.

896 Qi, W., Zhang, C., Fu, G., and Zhou, H.: Quantifying dynamic sensitivity of optimization
897 algorithm parameters to improve hydrological model calibration, Journal of Hydrology,
898 533, 213-223, 10.1016/j.jhydrol.2015.11.052, 2016.

899 Rodell, M., Houser, P. R., Jambor, U., Gottschalck, J., Mitchell, K., Meng, C. J., Arsenault,
 900 K., Cosgrove, B., Radakovich, J., Bosilovich, M., Entin*, J. K., Walker, J. P., Lohmann,
 901 D., and Toll, D.: The Global Land Data Assimilation System, Bulletin of the American
 902 Meteorological Society, 85, 381-394, 10.1175/bams-85-3-381, 2004.

903 Sapriza-Azuri, G., Jódar, J., Navarro, V., Slooten, L. J., Carrera, J., and Gupta, H. V.: Impacts
 904 of rainfall spatial variability on hydrogeological response, Water Resources Research, 51,
 905 1300-1314, 10.1002/2014wr016168, 2015.

906 Sellers, P. J.: Modeling the Exchanges of Energy, Water, and Carbon Between Continents and
 907 the Atmosphere, Science, 275, 502-509, 10.1126/science.275.5299.502, 1997.

908 Sellers, P. J., Mintz, Y., Sud, Y. C., and Dalcher, A.: A Simple Biosphere Model (SIB) for Use
 909 within General Circulation Models, Journal of the Atmospheric Sciences, 43, 505-531,
 910 10.1175/1520-0469(1986)043<0505:ASBMFU>2.0.CO;2, 1986.

911 Sellers, P. J., Randall, D. A., Collatz, G. J., Berry, J. A., Field, C. B., Dazlich, D. A., Zhang,
 912 C., Collelo, G. D., and Bounoua, L.: A Revised Land Surface Parameterization (SiB2) for
 913 Atmospheric GCMS. Part I: Model Formulation, Journal of Climate, 9, 676-705,
 914 10.1175/1520-0442(1996)009<0676:ARLSPF>2.0.CO;2, 1996.

915 Serpetzoglou, E., Anagnostou, E. N., Papadopoulos, A., Nikolopoulos, E. I., and Maggioni, V.:
 916 Error Propagation of Remote Sensing Rainfall Estimates in Soil Moisture Prediction from
 917 a Land Surface Model, Journal of Hydrometeorology, 11, 705-720,
 918 10.1175/2009jhm1166.1, 2010.

919 Shou, Y., and Xu, J.: The rainstorm and mesoscale convective systems over northeast China

920 in June 2005 I: A synthetic analysis of MCS by conventional observations and satellite data
 921 (in Chinese), *Acta Meteorologica Sinica*, 65, 160-170, 2007a.

922 Shou, Y., and Xu, J.: The rainstorm and mesoscale convective systems over northeast China
 923 in June 2005 II: A synthetic analysis of MCS's dynamical structure by radar and satellite
 924 observations (in Chinese), *Acta Meteorologica Sinica*, 65, 171-182, 2007b.

925 Shrestha, M., Wang, L., Koike, T., Tsutsui, H., Xue, Y., and Hirabayashi, Y.: Correcting
 926 basin-scale snowfall in a mountainous basin using a distributed snowmelt model and
 927 remote sensing data, *Hydrol. Earth Syst. Sci. Discuss.*, 10, 11711-11753,
 928 10.5194/hessd-10-11711-2013, 2013.

929 Sorooshian, S., Gao, X., Hsu, K., Maddox, R. A., Hong, Y., Gupta, H. V., and Imam, B.:
 930 Diurnal Variability of Tropical Rainfall Retrieved from Combined GOES and TRMM
 931 Satellite Information, *Journal of Climate*, 15, 983-1001,
 932 10.1175/1520-0442(2002)015<0983:DVOTRR>2.0.CO;2, 2002.

933 Sorooshian, S., Hsu, K. L., Gao, X., Gupta, H. V., Imam, B., and Braithwaite, D.: Evaluation
 934 of PERSIANN system satellite-based estimates of tropical rainfall, *Bulletin of the*
 935 *American Meteorological Society*, 81, 2035-2046,
 936 10.1175/1520-0477(2000)081<2035:eopsse>2.3.co;2, 2000.

937 Sorooshian, S., Lawford, R. G., Try, P., Rossow, W., Roads, J., Polcher, J., Sommeria, G., and
 938 Schifer, R.: Water and energy cycles: Investigating the links, *WMO Bull.*, 54, 2005.

939 Su, F., Hong, Y., and Lettenmaier, D. P.: Evaluation of TRMM Multisatellite Precipitation
 940 Analysis (TMPA) and Its Utility in Hydrologic Prediction in the La Plata Basin, *Journal*

941 of Hydrometeorology, 9, 622-640, 10.1175/2007jhm944.1, 2008.

942 Tapiador, F. J., Turk, F. J., Petersen, W., Hou, A. Y., García-Ortega, E., Machado, L. A. T.,
 943 Angelis, C. F., Salio, P., Kidd, C., Huffman, G. J., and de Castro, M.: Global precipitation
 944 measurement: Methods, datasets and applications, Atmospheric Research, 104-105, 70-97,
 945 10.1016/j.atmosres.2011.10.021, 2012.

946 Tolson, B. A., and Shoemaker, C. A.: Dynamically dimensioned search algorithm for
 947 computationally efficient watershed model calibration, Water Resources Research, 43,
 948 10.1029/2005wr004723, 2007.

949 Vrugt, J. A., ter Braak, C. J. F., Gupta, H. V., and Robinson, B. A.: Equifinality of formal
 950 (DREAM) and informal (GLUE) Bayesian approaches in hydrologic modeling?,
 951 Stochastic Environmental Research and Risk Assessment, 23, 1011-1026,
 952 10.1007/s00477-008-0274-y, 2009b.

953 Wang, D., Wang, G., and Anagnostou, E. N.: Use of Satellite-Based Precipitation Observation
 954 in Improving the Parameterization of Canopy Hydrological Processes in Land Surface
 955 Models, Journal of Hydrometeorology, 6, 745-763, 10.1175/JHM438.1, 2005.

956 Wang, F., Wang, L., Koike, T., Zhou, H., Yang, K., Wang, A., and Li, W.: Evaluation and
 957 application of a fine-resolution global data set in a semiarid mesoscale river basin with a
 958 distributed biosphere hydrological model, Journal of Geophysical Research, 116,
 959 10.1029/2011jd015990, 2011.

960 Wang, F., Wang, L., Zhou, H., Saavedra Valeriano, O. C., Koike, T., and Li, W.: Ensemble
 961 hydrological prediction-based real-time optimization of a multiobjective reservoir during

962 flood season in a semiarid basin with global numerical weather predictions, *Water*
 963 *Resources Research*, 48, 10.1029/2011wr011366, 2012.

964 Wang, L., Koike, T., Yang, D. W., and Yang, K.: Improving the hydrology of the Simple
 965 Biosphere Model 2 and its evaluation within the framework of a distributed hydrological
 966 model, *Hydrological Sciences Journal-Journal Des Sciences Hydrologiques*, 54,
 967 989-1006, 10.1623/hysj.54.6.989, 2009a.

968 Wang, L., Koike, T., Yang, K., Jackson, T. J., Bindlish, R., and Yang, D.: Development of a
 969 distributed biosphere hydrological model and its evaluation with the Southern Great
 970 Plains Experiments (SGP97 and SGP99), *Journal of Geophysical Research*, 114,
 971 10.1029/2008jd010800, 2009b.

972 Wang, L., Koike, T., Yang, K., Jin, R., and Li, H.: Frozen soil parameterization in a
 973 distributed biosphere hydrological model, *Hydrol. Earth Syst. Sci.*, 14, 557-571,
 974 10.5194/hess-14-557-2010, 2010a.

975 Wang, L., Koike, T., Yang, K., and Yeh, P. J.-F.: Assessment of a distributed biosphere
 976 hydrological model against streamflow and MODIS land surface temperature in the upper
 977 Tone River Basin, *Journal of Hydrology*, 377, 21-34, 10.1016/j.jhydrol.2009.08.005,
 978 2009c.

979 Wang, L., Wang, Z., Koike, T., Yin, H., Yang, D., and He, S.: The assessment of surface water
 980 resources for the semi-arid Yongding River Basin from 1956 to 2000 and the impact of
 981 land use change, *Hydrological Processes*, 24, 1123-1132, 10.1002/hyp.7566, 2010b.

982 Xie, P., Chen, M., Yang, S., Yatagai, A., Hayasaka, T., Fukushima, Y., and Liu, C.: A

983 Gauge-Based Analysis of Daily Precipitation over East Asia, Journal of
984 Hydrometeorology, 8, 607-626, 10.1175/jhm583.1, 2007.

985 Xue, X., Hong, Y., Limaye, A. S., Gourley, J. J., Huffman, G. J., Khan, S. I., Dorji, C., and
986 Chen, S.: Statistical and hydrological evaluation of TRMM-based Multi-satellite
987 Precipitation Analysis over the Wangchu Basin of Bhutan: Are the latest satellite
988 precipitation products 3B42V7 ready for use in ungauged basins?, Journal of Hydrology,
989 499, 91-99, 10.1016/j.jhydrol.2013.06.042, 2013.

990 Yang, D.: Distributed hydrological model using hillslope discretization based on catchment
991 area function: development and applications, PHD, University of Tokyo, Tokyo, 1998.

992 Yang, K., Koike, T., and Ye, B.: Improving estimation of hourly, daily, and monthly solar
993 radiation by importing global data sets, Agricultural and Forest Meteorology, 137, 43-55,
994 10.1016/j.agrformet.2006.02.001, 2006.

995 Yatagai, A., Kamiguchi, K., Arakawa, O., Hamada, A., Yasutomi, N., and Kitoh, A.:
996 APHRODITE: Constructing a Long-Term Daily Gridded Precipitation Dataset for Asia
997 Based on a Dense Network of Rain Gauges, Bulletin of the American Meteorological
998 Society, 93, 1401-1415, 10.1175/bams-d-11-00122.1, 2012.

999 Yong, B., Chen, B., Gourley, J. J., Ren, L., Hong, Y., Chen, X., Wang, W., Chen, S., and Gong,
1000 L.: Intercomparison of the Version-6 and Version-7 TMPA precipitation products over
1001 high and low latitudes basins with independent gauge networks: Is the newer version
1002 better in both real-time and post-real-time analysis for water resources and hydrologic
1003 extremes?, Journal of Hydrology, 508, 77-87, 10.1016/j.jhydrol.2013.10.050, 2014.

1004 Yong, B., Hong, Y., Ren, L.-L., Gourley, J. J., Huffman, G. J., Chen, X., Wang, W., and Khan,
 1005 S. I.: Assessment of evolving TRMM-based multisatellite real-time precipitation
 1006 estimation methods and their impacts on hydrologic prediction in a high latitude basin,
 1007 Journal of Geophysical Research, 117, 10.1029/2011jd017069, 2012.

1008 Yong, B., Ren, L.-L., Hong, Y., Wang, J.-H., Gourley, J. J., Jiang, S.-H., Chen, X., and Wang,
 1009 W.: Hydrologic evaluation of Multisatellite Precipitation Analysis standard precipitation
 1010 products in basins beyond its inclined latitude band: A case study in Laohahe basin, China,
 1011 Water Resources Research, 46, 10.1029/2009wr008965, 2010.

1012 Yuan, M., Li, Z., and Zhang, X.: Analysis of a meso scale convective system during a brief
 1013 torrential rain event in Northeast China (in Chinese), Acta Meteorologica Sinica, 68,
 1014 125-136, 10.11676/qxxb2010.013, 2010.

1015 Zhao, T., and Yatagai, A.: Evaluation of TRMM 3B42 product using a new gauge-based
 1016 analysis of daily precipitation over China, International Journal of Climatology, 34,
 1017 2749-2762, 10.1002/joc.3872, 2014.

1018 Zhou, T., Yu, R., Chen, H., Dai, A., and Pan, Y.: Summer Precipitation Frequency, Intensity,
 1019 and Diurnal Cycle over China: A Comparison of Satellite Data with Rain Gauge
 1020 Observations, Journal of Climate, 21, 3997-4010, 10.1175/2008jcli2028.1, 2008.

1021 Zhou, X. Y., Zhang, Y. Q., Yang, Y. H., Yang, Y. M., and Han, S. M.: Evaluation of anomalies
 1022 in GLDAS-1996 dataset, Water Science and Technology, 67, 1718-1727,
 1023 10.2166/wst.2013.043, 2013.

1024

1025 Table 1 Precipitation products

Product	Spatial resolution	Temporal resolution	Areal coverage	Start date	Type
TRMM3B42	0.25°	3h	Global 50°N-S	1 Jan 1998	PR+IR+MW+gauge+HM
TRMM3B42RT	0.25°	3h	Global 50°N-S	1 Mar 2000	IR+MW
GLDAS/Noah	0.25°	3h	Global 90°N-60°S	24 Feb 2000	IR+MW+gauge
GSMAP-MVK+	0.1°	1h	Global 60°N-S	1 Mar 2000	IR+MW+CMV
PRRSIANN	0.25°	3h	Global 60°N-S	1 Mar 2000	PR+IR+MW+ANN
APHRODITE	0.25°	1day	60°E-150°E, 15°S-55°N	1 Jan 1961 to 2007	gauge

1026 PR: precipitation radar; IR: infrared estimation; MW: microwave estimation; HM: histogram

1027 matching; CMV: cloud motion vectors; ANN: artificial neural network.

1028

1029 Table 2 WEB-DHM parameters

Symbol (unit)	Brief description	Basin-averaged value
<i>KS</i> (mm/h)	Saturated hydraulic conductivity for soil surface	26.43
<i>Anik</i>	Hydraulic conductivity anisotropy ratio	11.49
<i>Sstmax</i> (mm)	Maximum surface water storage	42.75
<i>Kg</i> (mm/h)	Hydraulic conductivity for groundwater	0.36
<i>alpha</i>	van Genuchten parameter	0.01
<i>n</i>	van Genuchten parameter	1.88

1030

1031 Table 3 TOPMODEL parameters

Name (unit)	Description	Lower bound	Upper bound	Calibration
SZM (m)	form of the exponential decline in conductivity	0.01	0.04	0.019
$LNT0$ (m ² h ⁻¹)	log value of effective lateral saturated transmissivity	-25	1	-11.911
RV (m h ⁻¹)	hill slope routing velocity	2000	5000	2608.4
SR_{max} (m)	maximum root zone storage	0.001	0.01	0.006
SR_0 (m)	initial root zone deficit	0	0.01	0.005
TD (m h ⁻¹)	unsaturated zone time delay per unit deficit	2	4	2.885

1032

1033

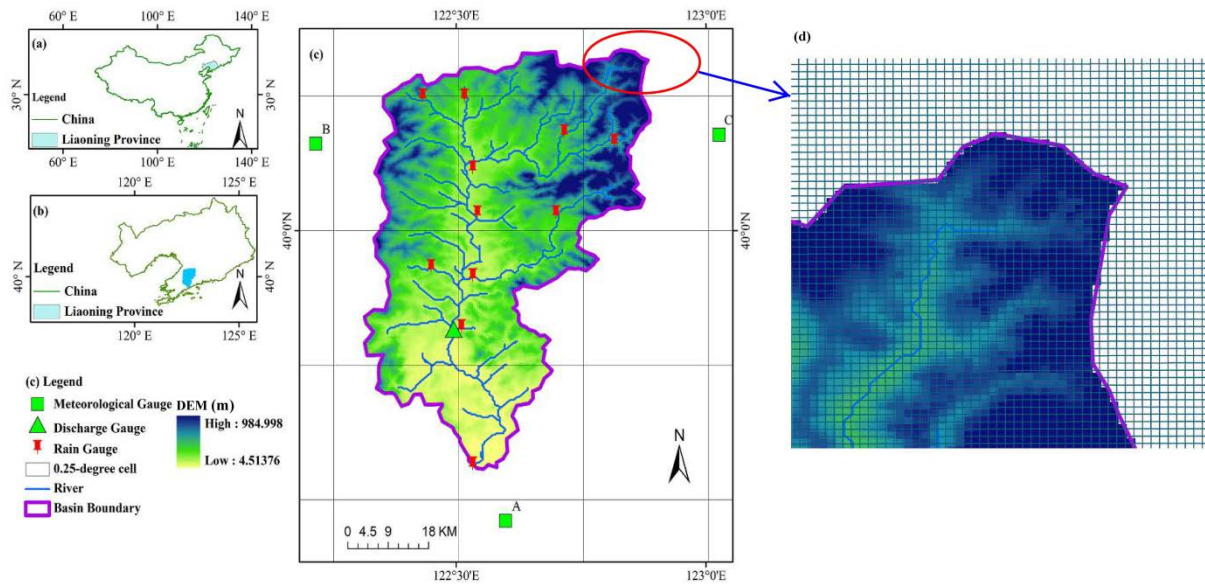


Fig. 1 Biliu basin: (a) the location of Liaoning province within China; (b) the location of Biliu basin within Liaoning province; (c) the distributions of rain gauges, discharge gauge, automatic weather stations, digital elevation model, and diagrammatic 0.25-degree precipitation cells; and (d) diagrammatic description of downscaling the 0.25-degree precipitation cells to 300 m × 300 m cells, and retrieving the 300 m × 300 m cells located within the basin boundary.

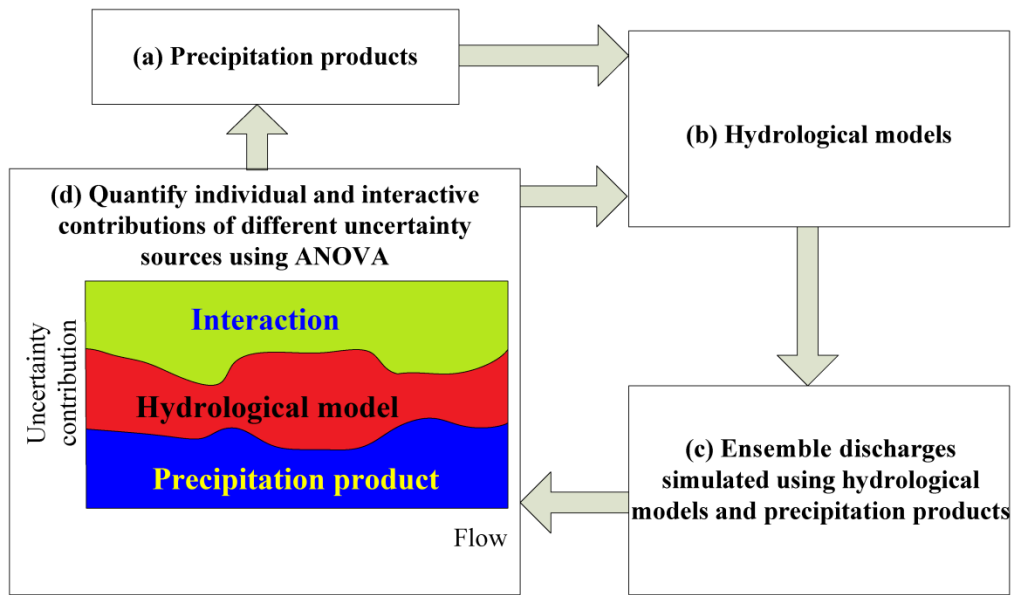


Fig. 2 Diagrammatic flowchart of the proposed framework for quantification of uncertainty contributions to ensemble discharges simulated using precipitation products on the basis of the analysis of variance (ANOVA) approach.

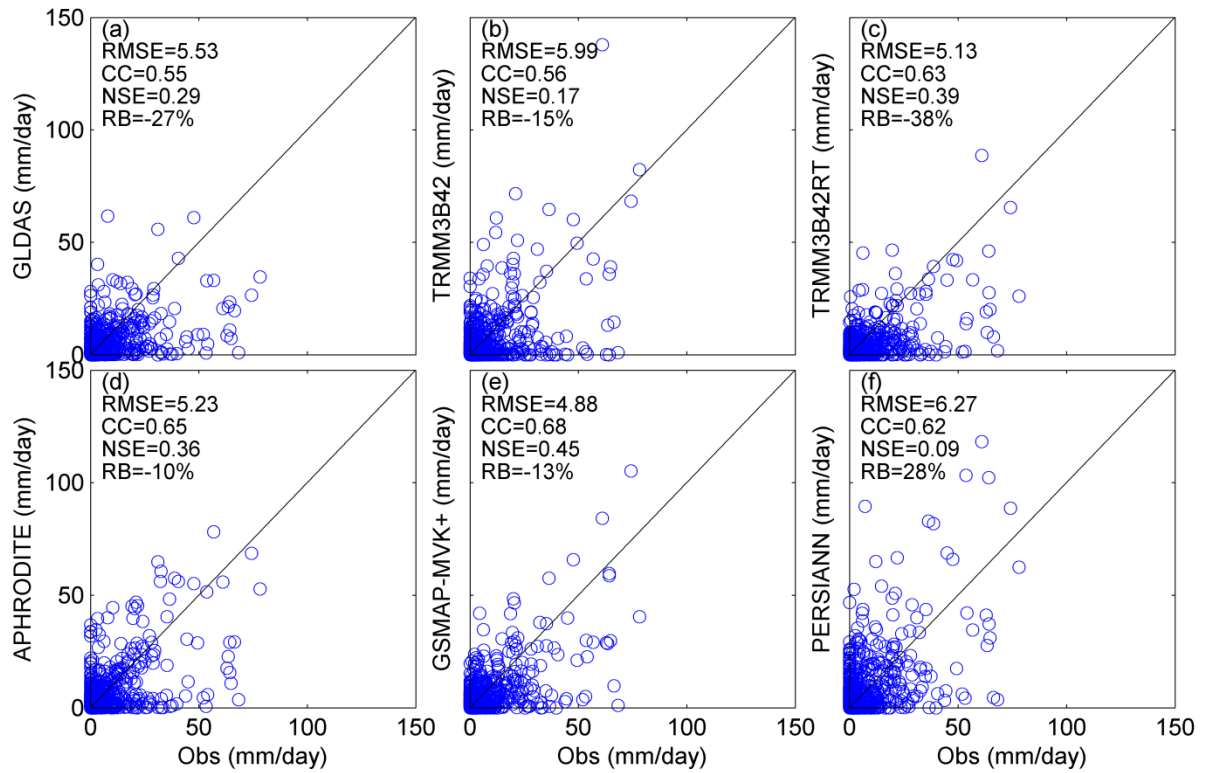


Fig. 3 Scatterplots of basin-averaged precipitation products versus gauge observations at a daily scale.

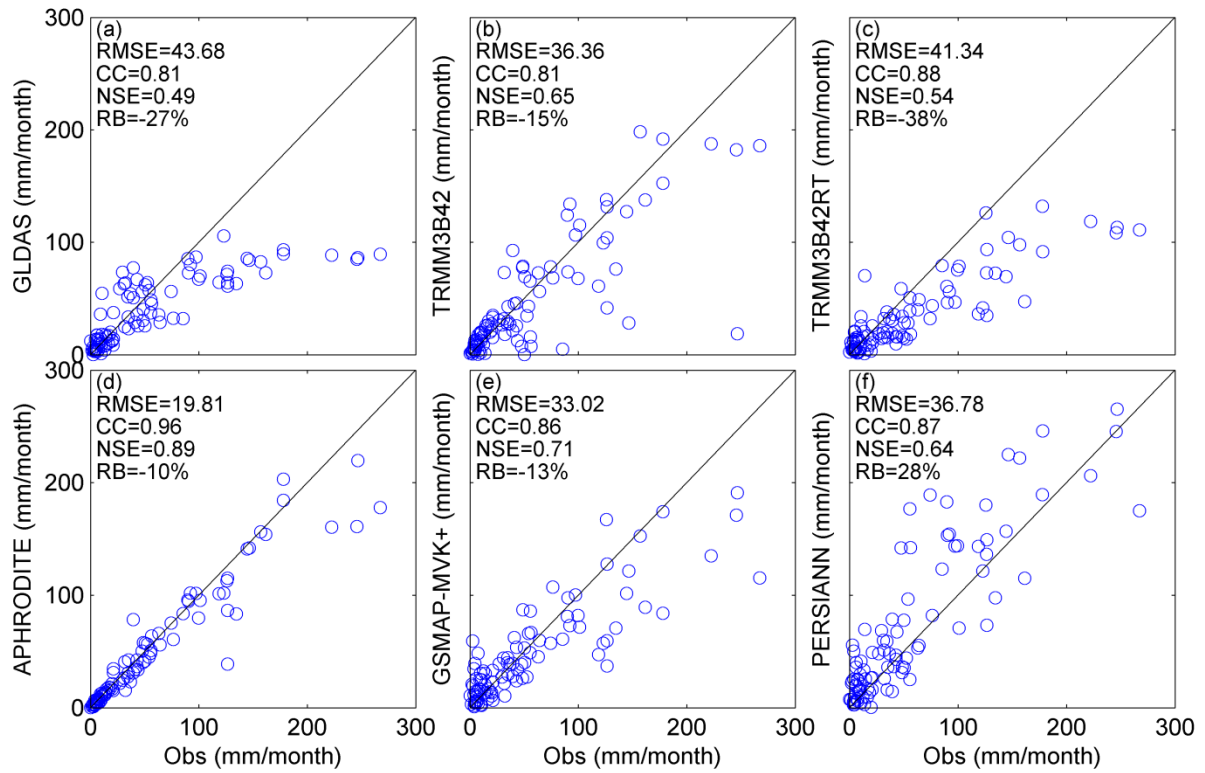


Fig. 4 Scatterplots of basin-averaged precipitation products versus gauge observations at a monthly scale.

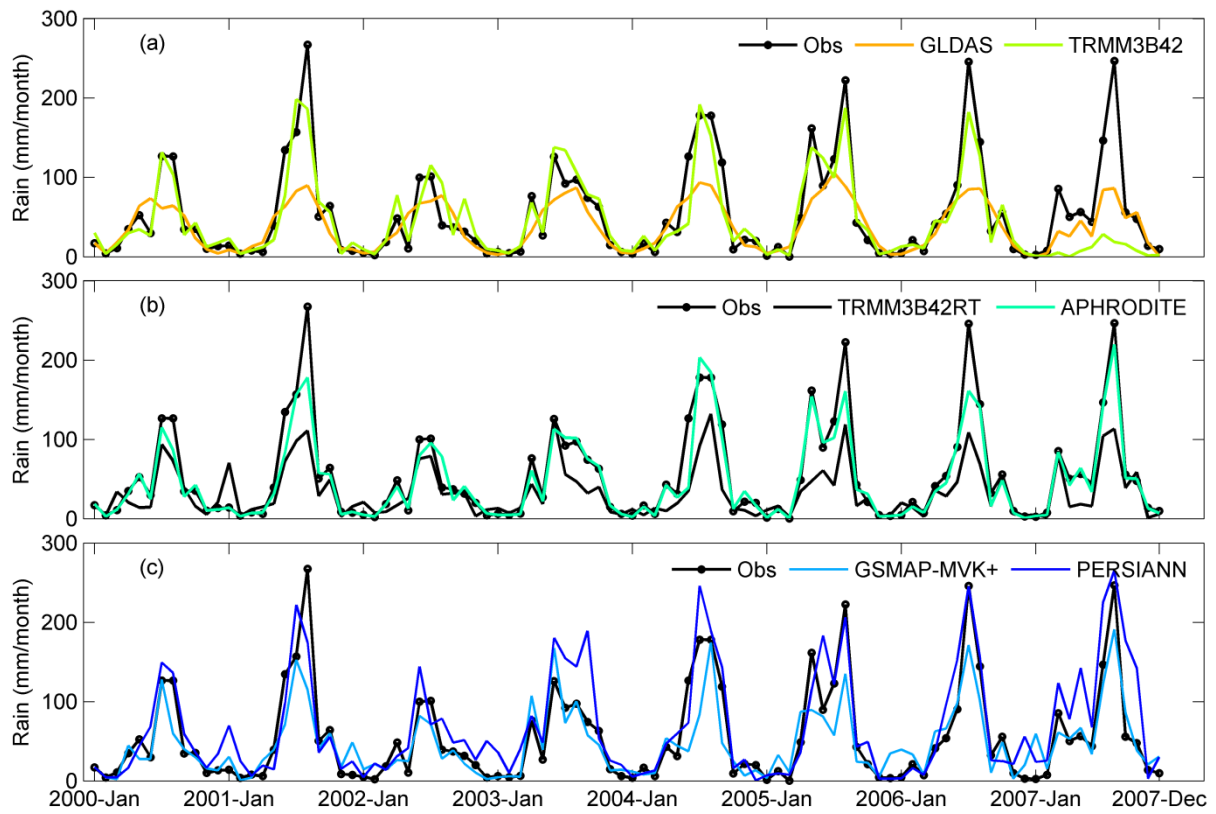


Fig. 5 Time series plots of basin-averaged precipitation product values versus gauge observations at monthly scale.

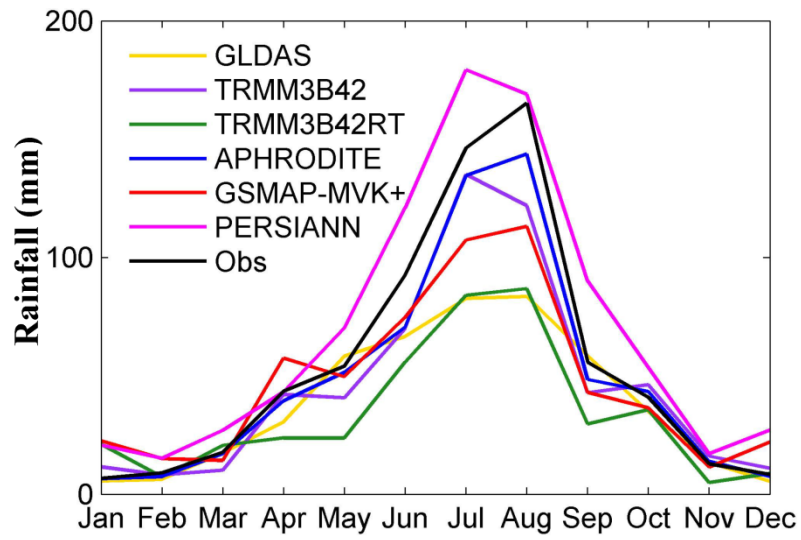


Fig. 6 Inter-annual basin-averaged monthly precipitation.

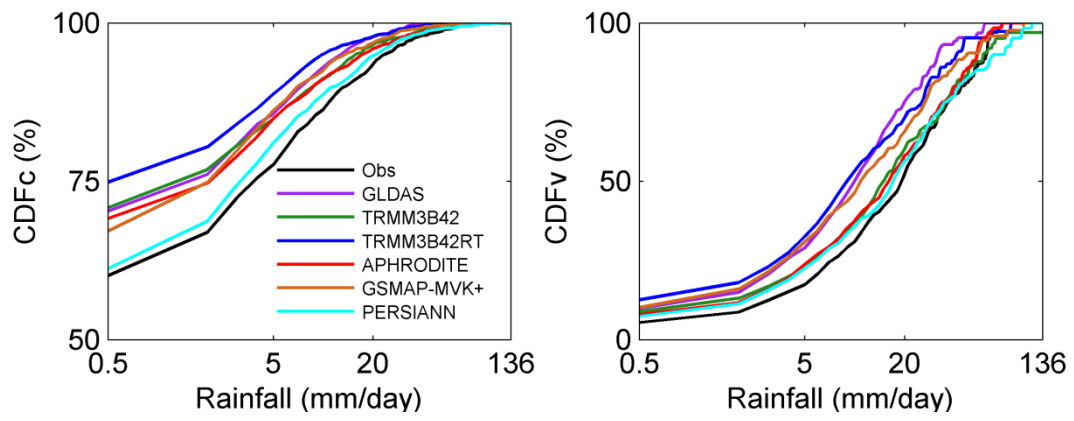


Fig. 7 Probability distributions of the six precipitation products by occurrence (CDFc) and volume (CDFv).

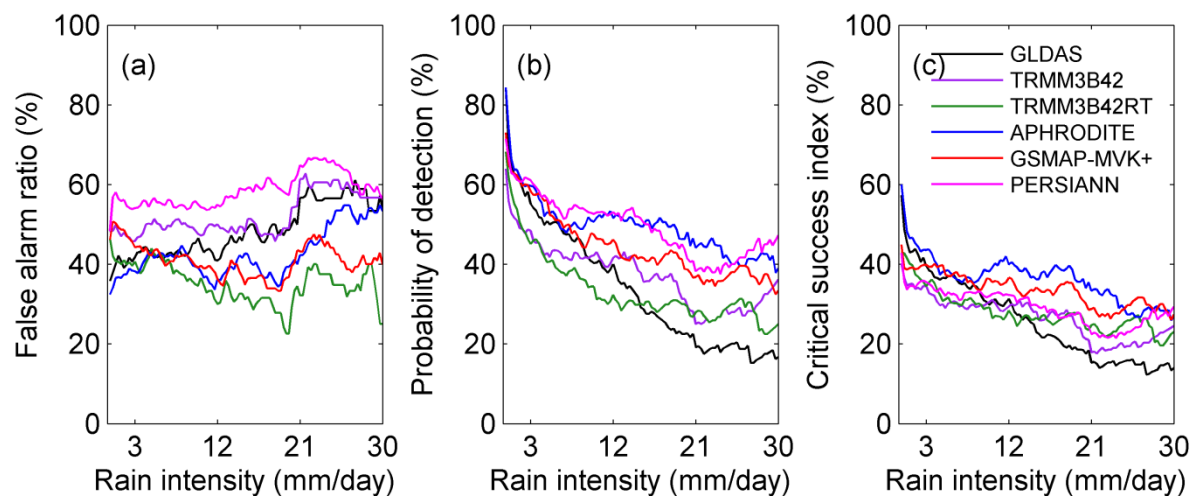


Fig. 8 False alarm ratio, probability of detection and critical success index for the six precipitation products.

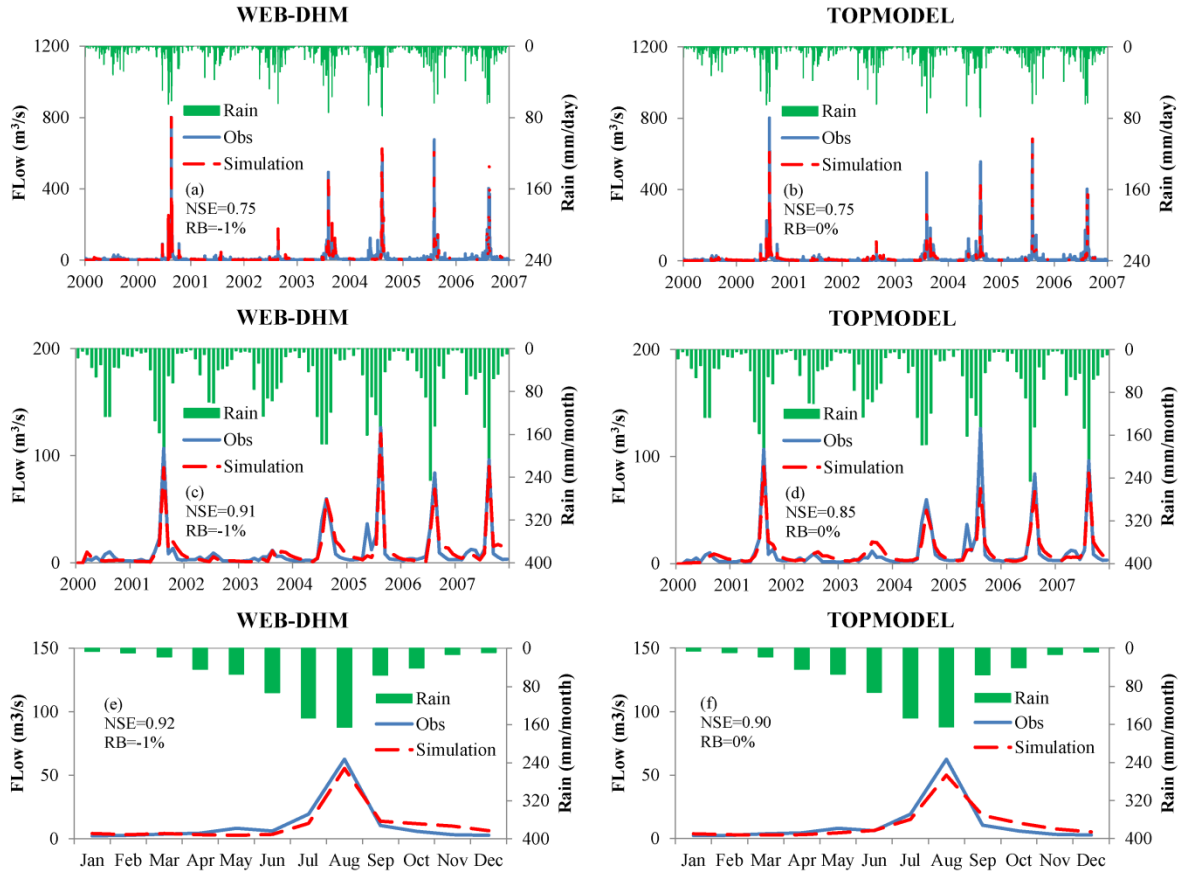


Fig. 9 Observed and simulated flows using WEB-DHM and TOPMODEL from 2000 to 2007: (a), (c) and (e) are daily, monthly and inter-annual simulations using WEB-DHM respectively; (b), (d) and (f) are daily, monthly and inter-annual simulations using TOPMODEL respectively.

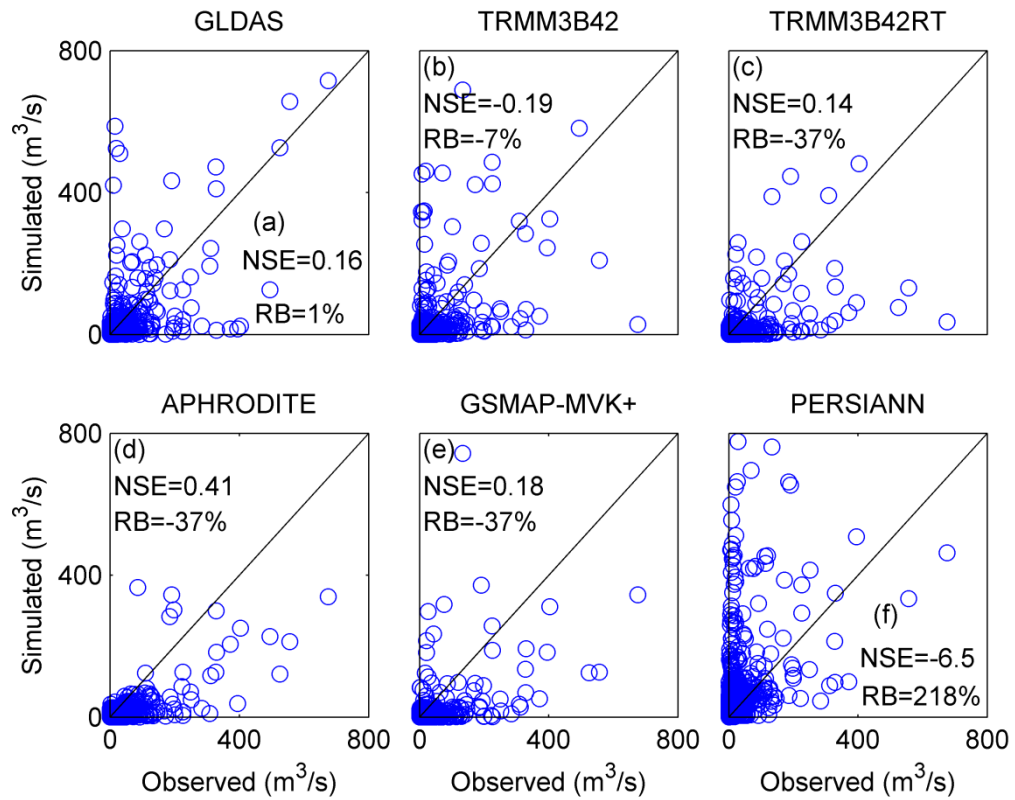


Fig. 10 Scatterplots of simulated discharges with WEB-DHM against gauge observations at a daily scale.

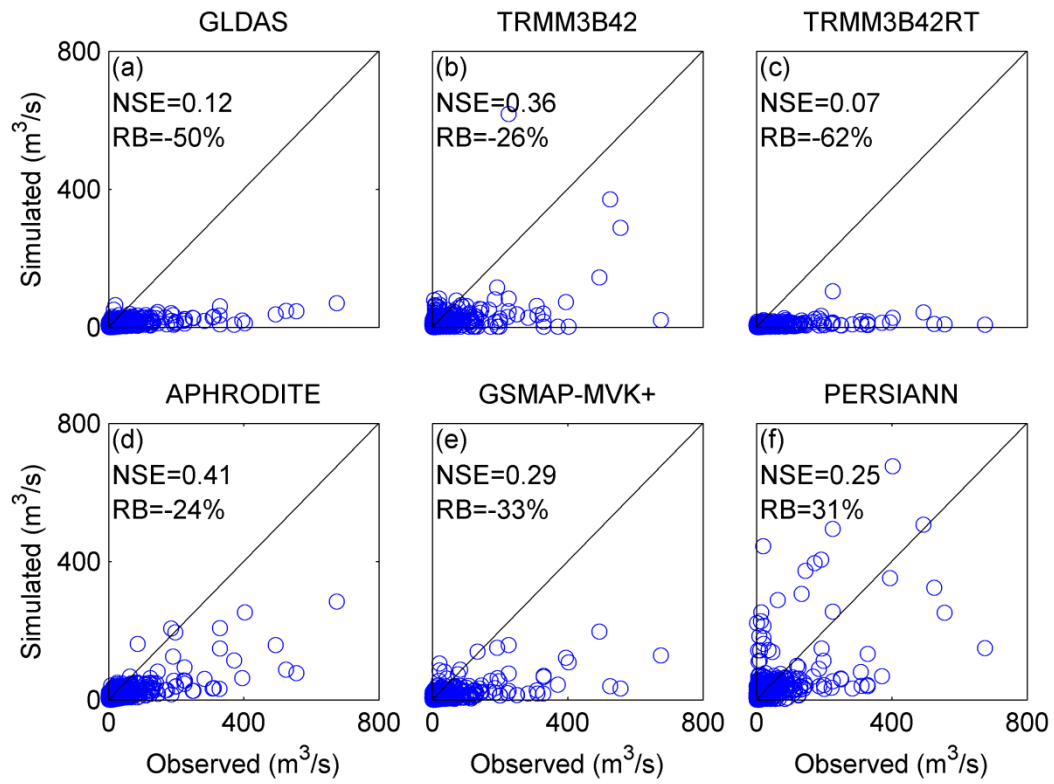


Fig. 11 Scatterplots of simulated discharges with TOPMODEL against gauge observations at a daily scale.

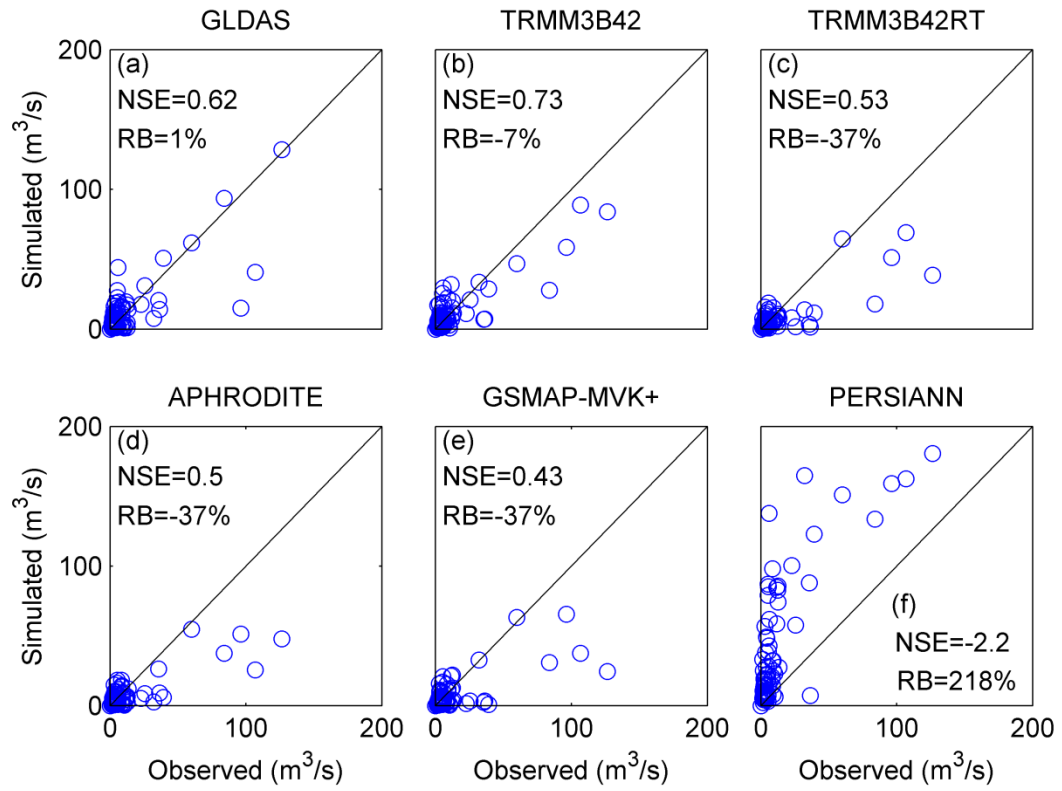


Fig. 12 Scatterplots of simulated flows with WEB-DHM against gauge observations at a monthly scale.

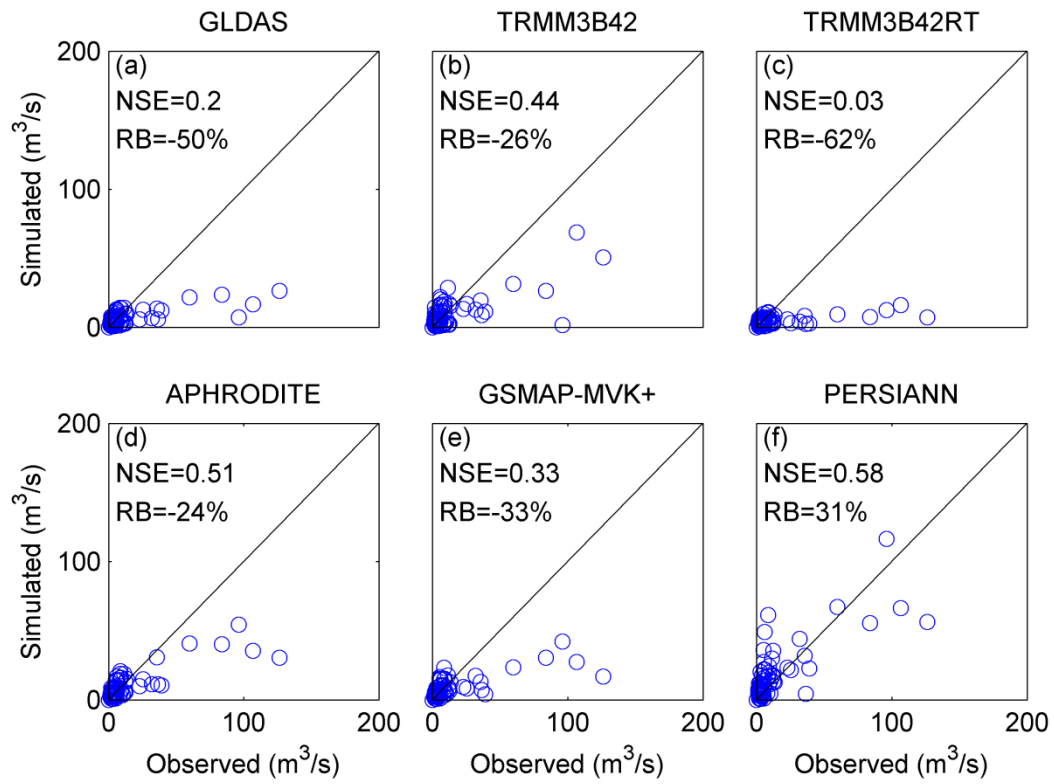


Fig. 13 Scatterplots of simulated discharges with TOPMODEL against gauge observations at a monthly scale.

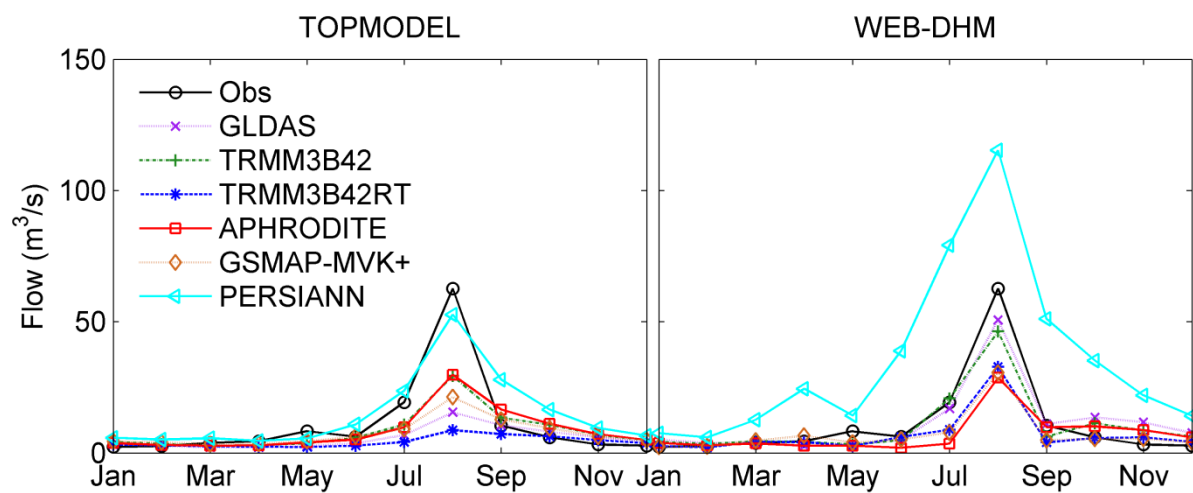


Fig. 14 Inter-annual average monthly discharges.

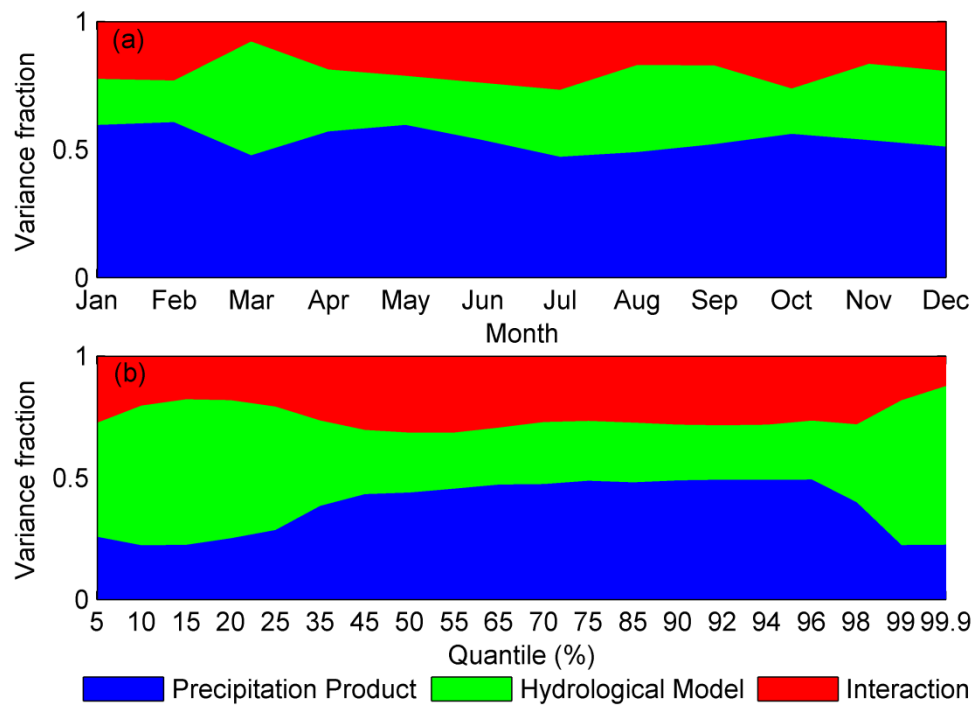


Fig. 15 Contributions of uncertainty sources to (a) average monthly discharges and (b) discharge quantiles based on daily scale simulated results.